Master's thesis

NTNU
Norwegian University of Science and Technology
Faculty of Engineering

Druesnes, Karl

Revealing the role of hydroxyl groups in the adhesive properties of DOPA derivatives

Master's thesis in Nanomechanics
Supervisor: Xiao, Senbo
Co-supervisor: Rothmund, Erling V.
June 2023

NTNU
Norwegian University of
Science and Technology

Druesnes, Karl

Revealing the role of hydroxyl groups in the adhesive properties of DOPA derivatives

Master's thesis in Nanomechanics
Supervisor: Xiao, Senbo
Co-supervisor: Rothmund, Erling V.
June 2023

Norwegian University of Science and Technology
Faculty of Engineering

NTNU
Norwegian University of
Science and Technology

Abstract

Among all the natural adhesive materials, it is known that polyphenols are the common chemical ingredients playing a significant role in the adhesive properties. More especially, the crucial chemical structure of natural adhesive materials consists of benzene ring derivatives with varied number of hydroxyl groups.

DOPA derivatives materials with varied number of hydroxyl groups have been studied with molecular dynamics simulations in three different structures: as a bulk, as a layer and as a solvated layer. The software Gromacs provided data about H-bonds and energies within the systems, meanwhile the conformation of the interacting molecules was studied using Python.

This work highlights the key roles played by hydroxyl groups in DOPA derivatives materials which are to actively participate in forming H-bonds and to bind the systems, shortening the length of H-bonds, the distance between interacting benzenes, and affecting the potentials in the systems and the molecules conformation. The irregularities among the different hydroxyl groups impacts are also underlined thorough the results.

The conclusions of this study demonstrate the important role of hydroxyl groups on the adhesive properties of DOPA derivatives materials by focusing on the side chain of monomers and it would be interesting to extend these results by the study of long chains of polymers.

Sammendrag

Blant alle naturlige klebematerialer er det kjent at polyfenoler er de vanlige kjemiske ingrediensene som spiller en betydelig rolle i klebeegenskapene. Mer spesifikt består den avgjørende kjemiske strukturen til naturlige klebematerialer av benzenringderivater med varierende antall hydroksylgrupper.

DOPA-derivater med varierende antall hydroksylgrupper har blitt studert med molekylær dynamikk-simuleringer i tre forskejellige strukturer: som et bulkmateriale, som et lag og som et løsningsmiddellag. Programvaren Gromacs har gitt data om H-bindinger og energi innenfor systemene, samtidig som konformasjonen til de interagerende molekylene ble studert ved hjelp av Python.

Dette arbeidet fremhever de viktige rollene som hydroksylgrupper i DOPA-derivater spiller, nemlig å aktiv deltai dannelse av H-bindinger og å binde systemene sammen, forkorte lengden på H-bindinger, avstanden mellom interagerende benzenforbindelser og påvirke potensialene i systemene og konformasjonen av molekylene. Ujevnhetene blant de ulike hydroksylgruppenes påvirkning blir også understreket gjennom resultatene.

Resultatene i denne studien viser den viktige rollen som hydroksylgrupper spiller for klebeegenskapene til DOPA-derivater ved å fokusere på sidekjeden til monomerene, og det ville være interessant å utvide disse resultatene ved å studere lange polymerkjeder.

Preface

This master thesis has been written under the supervision of Professor Senbo Xiao and Erling V. Rothmund in the Department of Structural Engineering in NTNU.

I would like to express my gratitude to Professor Senbo Xiao for his trust, availability, and willingness to help me improve my work. The systematic positive feedback and exchanges contributed to my good development during this semester.

I would also like to thank the Department's members for their welcome in the seminars which have enriched my thoughts.

I would like to thank Vilde Margrethe for her help in translating the abstract into Norwegian, the support and for all the moments we shared. As well as I am grateful to the friends I met here in NTNU and the rowing team.

Lastly, I am grateful to all of those who were involved directly and indirectly in the completion of my studies.

Table of Contents

List of Figures

List of Tables

List of Equations

List of Abbreviations (or Symbols)

NTNU	The Norwegian University of Science and Technology
MD	Molecular Dynamics
MFP	Mussel Foot Protein
DOPA	3,4-dihydroxyphenylalanine
0hydro	Phenylalanine
1hydro	Tyrosine 4-hydroxyphenylalanine
2hydro	DOPA 3,4-dihydroxyphenilalanine

3hydro	3,4,5-trihydroxyphenilalanine
Xhydro	Designates the four molecules from 0hydro to 3hydro
LJ	Lennard-Jones
EM	Energy minimization
NVT	Simulation in which the Number of particles, Volume and Temperature are constant
NPT	Simulation in which the Number of particles, Pressure and Temperature are constant
OPLS	Optimized Potentials for Liquid Simulations
SR	Short Range
SICD	Shortest Inter-residue C-C Distance
d	SICD Specified in the python analysis part
α	Angle Specified in the python analysis part
t	Duration of simulation
T	Temperature
P	Pressure

1 Introduction

1.1 Natural adhesive materials

Natural adhesive materials, especially the underwater adhesive of marine organisms and the tannin compounds from many plants, have been the focuses of biomimetics study in the past decade [1]. Among all the natural adhesive materials, it is known that polyphenols are the common chemical ingredients playing a significant role in the adhesive properties, as shown in Figure 1. More especially, the crucial chemical structure of natural adhesive materials consists of benzene ring derivatives with varied number of hydroxyl groups.

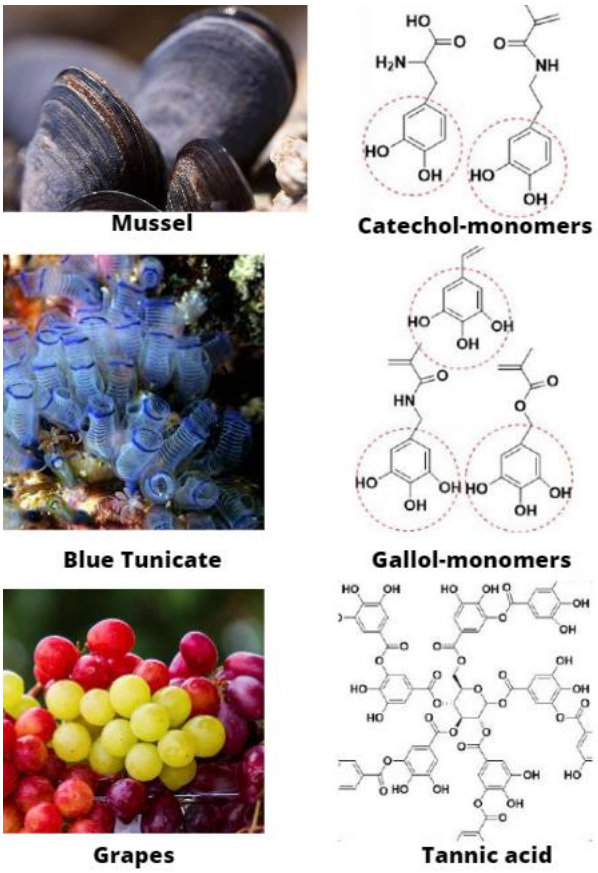

Figure 1 : Examples of adhesives proteins in nature

One of the most famous natural adhesive materials is the adhesive protein in the mussel foot [2]. The adhesion mechanism of the mussel adhesive protein, or mussel foot proteins (MFPs), had been in-depth investigated by [3]. It describes the molecular organization of a mussel foot and the chemical reactions and processes that take place to set up the adhesion of the mussel to the substrate. A better understanding of these mechanisms could lead to many applications because of the great strength and moisture-resistance of the bonding. The understanding of the adhesion mechanism of mussel adhesive protein is also critically important for anti-biofouling, which could shed light on the improvement of the

coating industry for boat hull [4]. Furthermore, applying the adhesion mechanism of mussel foot could also be at the guidelines in new biomimetic materials synthesis for biomedical or other industrial applications [5].

There are six different mussel foot proteins (MFPs) identified today, with their spatial organization, indicated Figure 2, and their chemical roles in the attachment process. One of the unique features of MFPs is the abundance of the catecholic amino acid, called DOPA, in their protein sequences, as the chemical structure of DOPA shown in Figure 3. Specifically, a DOPA monomer is made of a catechol sidechain two hydroxyl groups attached to the benzene ring, and other groups with O and N atoms on the backbone. The presence of catechol is believed to fulfill the dual role of interfacial bonding and the solidification of the adhesive proteins. Comparing the amino acid monomer tyrosine (Figure 3), the extra hydroxyl group in the catechol of DOPA is the key to its extraordinary adhesive properties [3]. It is thus interesting to speculate the effect of different number of hydroxyl group in determining the adhesion performance of mussel-foot-protein-like (MFP-like) materials.

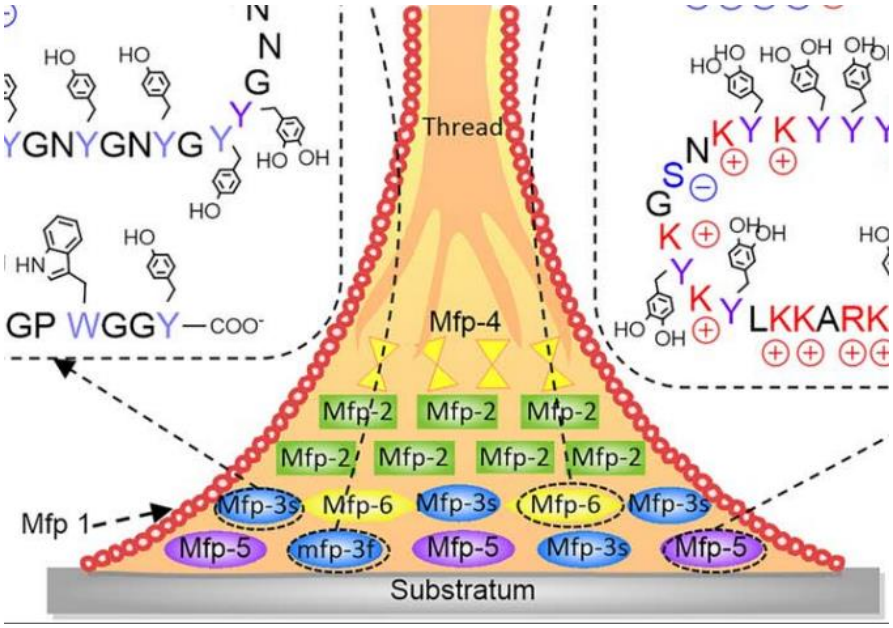

Figure 2 : MFPs schematic distribution in a mussel foot thread (readapted from [3])

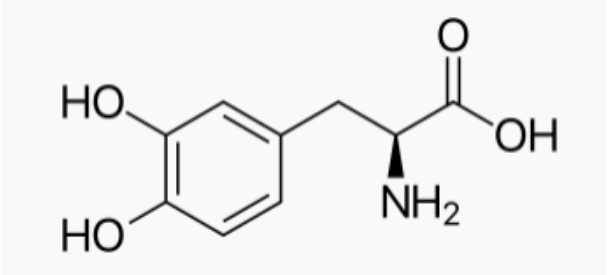

(a)

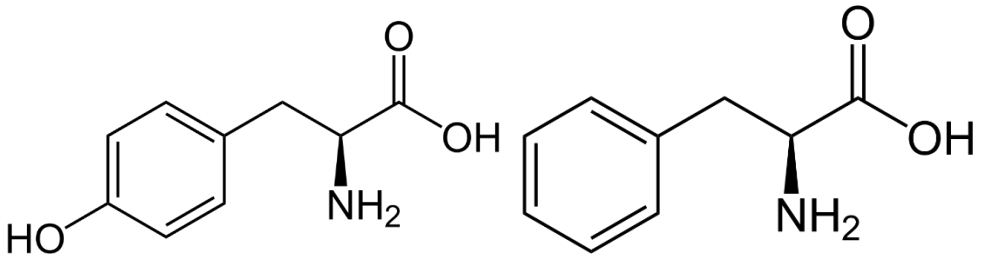

(b) **(c)**

Figure 3 : (a) DOPA, 3,4-dihydroxyphenylalanine. (b) Tyrosine, 4-hydroxyphenylalanine. (c) Phenylalanine.

The benzene and the hydroxyl groups of catechol obviously have distinct functions. As shown in Figure 4, the benzene ring is at the heart of many interactions (covalent or non-covalent cross-linking) and reactions in its environment. The hydroxyl groups are likely to play a key role in all the non-covalent cross-linking, because of its dual properties of being both the donor and the accepter of hydrogen bonding. However, the benzene ring can interact with other rings through π-π electron interaction or with positively charged ions through cation-π interaction [6]. More details about these interactions are given in the following chapter.

As example by comparing DOPA and tyrosine monomers above, the modification of one extra hydroxyl group on the benzene ring of tyrosine leads to substantial changes in physical and chemical in the properties of the MFPs. It is thus intriguing to understand the properties of MFP-like materials with further extra hydroxyl group or no hydroxyl group at all.

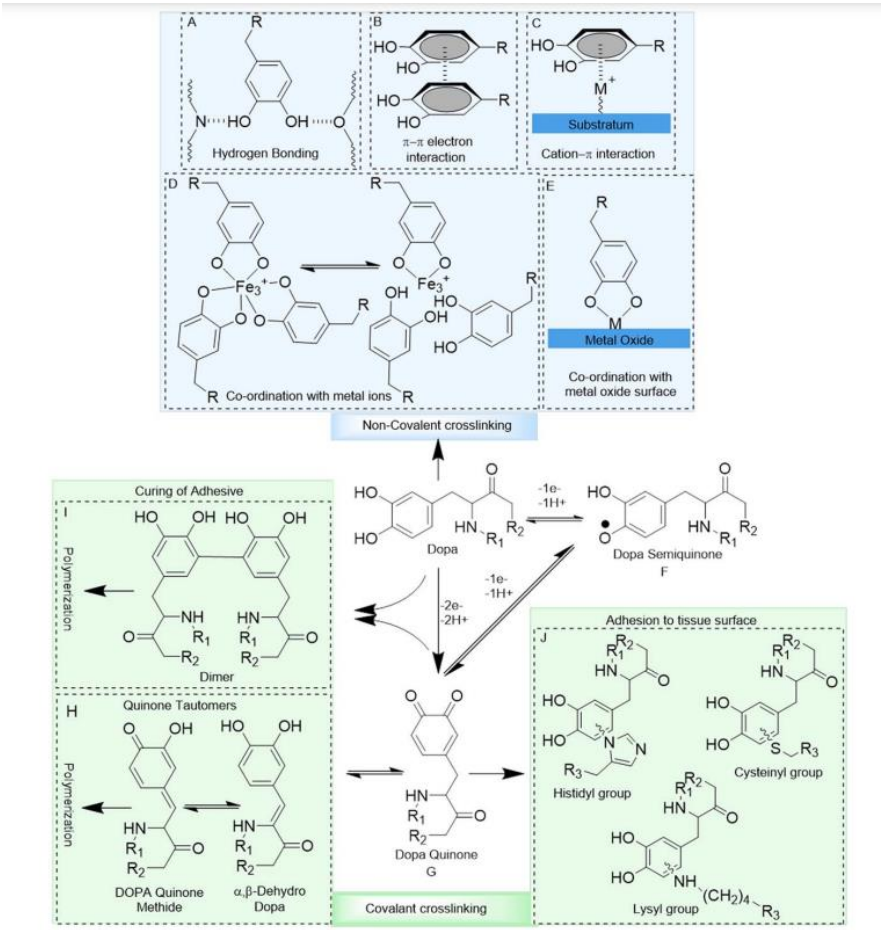

Figure 4 : Interactions and reaction products of the catechol side chain of DOPA

This master thesis focuses on atomistic modeling and molecular dynamics (MD) simulations of DOPA derivatives with varied number of hydroxyl groups, devoting to dissect the key molecular ingredients of adhesive performance of the materials. Specifically, the following DOPA derivatives with varied hydroxyl groups are first modeled: phenylalanine, tyrosine, DOPA (Figure 3) and 3,4,5-trihydroxyphenilalanine. To make this report more understandable, we call these molecules respectively 0hydro, 1hydro, 2hydro and 3hydro according to their number of hydroxyl groups. The four derivatives are subjected molecular dynamics (MD) simulation to the investigation of their molecular compact ability, their interface properties with and without water environment. The results of this master thesis will provide the molecular basis for the understanding of the determining roles of hydroxyl groups and benzene in MFP-like materials.

1.2 Atomistic parameter and MD Simulation

For carrying out calculations related to this master thesis, the super-computer Sigma2 in the Norwegian research infrastructure services were utilized. The selected method, MD simulations [7], is one of the most popular computational tools for investigating interactions and behaviors of molecules nowadays. This is a numerical simulation method allowing to model the movement of atoms and molecules over time and study the evolution of a system. The systems studied with MD simulation are normally very small, as well as the duration of the simulation. These two parameters have a major influence on the simulation time. The evolution of the system in MD simulation follows the Newton's equations of motion, in a given environment (temperature, pressure, boundary conditions,

electrostatic field…). MD simulation is used for multiple-particle systems which are too complex to be determined analytically. Of course, like as a numerical method, MD simulation makes assumptions and therefore approximations. These approximations can however be minimized by choosing the more adapted algorithms and settings for a given system [8]. To carry out all the MD simulations in this work, the software Gromacs (Version 2016.6) was used. Gromacs is a package mainly designed for simulations of proteins, nucleic acids and lipids [9]. This software was developed by the University of Groningen and is a free and open source. The main concepts useful for understanding this work are described in the following sub-sections.

1.2.1 Force Fields

A force field is a vector field corresponding with a non-contact force acting at various positions in space. So, a simple example of force field in Gromacs is the electrostatic field created by the atoms. Sets of force fields are already implemented in the software like *AMBER*, *CHARMM* or *GROMOS* [10]. The following section briefly introduces all the equations and atom parameters needed for our work.

The Coulombic force, also called electrostatic force, expresses the attractive or repulsive electric force between two charged bodies. For two charges of opposite signs, the force will be attractive and its value negative. This force is inversely proportional to the square of the distance r between them.

$$F_C = \frac{1}{4\pi\varepsilon_0} \cdot \frac{q_1 q_2}{r^2} = k_e \frac{q_1 q_2}{r^2}$$

Equation 1 : Coulombic force between two charged bodies

Where q1 and q2 are the magnitudes of the charges, ε_0 is the vacuum electric permittivity and $k_e = 8{,}988 \times 10^9 \ N.m^2.C^{-2}$.

Hence the electrical potential energy:

$$V_C = k_e \frac{q_1 q_2}{r}$$

Equation 2 : Coulombic Potential

The Lennard-Jones potential is an intermolecular pair potential used for simple yet realistic intermolecular interactions:

$$V_{LJ} = 4\varepsilon \left[\left(\frac{\sigma}{r}\right)^{12} - \left(\frac{\sigma}{r}\right)^{6} \right]$$

Equation 3 : Lennard-Jones Potential

Where σ is the distance at which the particle-particle potential energy is zero and ε is a potential energy such that, when the distance r between the two particles allows the Lennard-Jones potential to be at its minimum, the potential energy is V = -ε. See [11] for more details about the determination of the Lennard-Jones parameters.

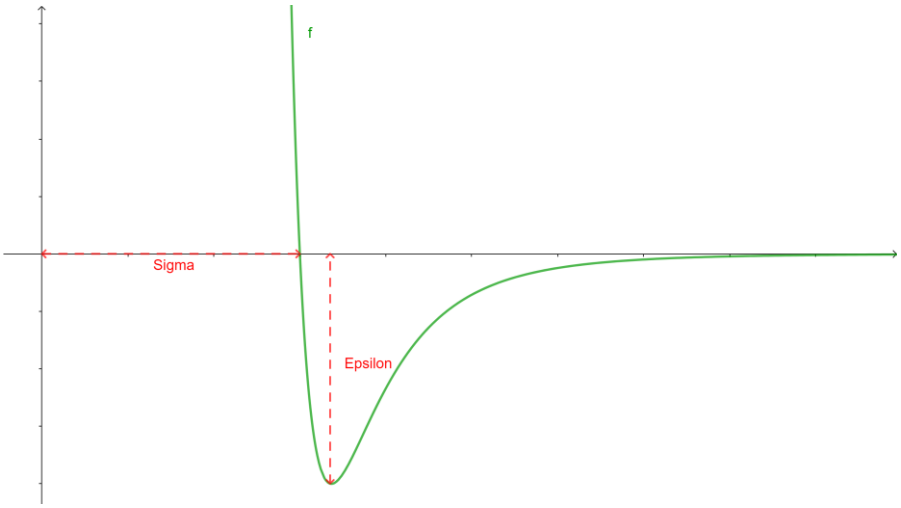

Figure 5 : Example of Lennard-Jones Potential curve

These potentials can be applied on all the pairs of atoms present in the system, whatever the distance between the two atoms. However, these potentials decay fast and the calculation of all the potentials in the system is not relevant as many are negligible. So, a cut-off is used in Gromacs to save calculation capacity and time. That is to say that for each atom, only the atoms that are close enough are considered in the calculation of potentials. The cut-off used in this work is 1.0 nm.

1.2.2 Hydrogen bond and hydroxyl group

The hydrogen bond or H-bond is an intermolecular or intramolecular attractive interaction between a hydrogen atom, covalently bound to an electronegative group or atom (the Donor), and a less electronegative atom (the Acceptor) [12]. Electronegativity (symbol χ) is a chemical property that describes the ability of an atom to attract electrons when forming a chemical bond. The higher the electronegativity, the more the atom or group attracts electrons to itself. For example, according to the Pauling scale, running from 0.79 to 3.98, we have in one hand the oxygen which is very electronegative $\chi_O = 3.44$ and in another hand lower electronegative hydrogen $\chi_H = 2.2$. The strength of the H-bond is weaker than a covalent bond but stronger than a van der Waals interaction. Nitrogen (N), oxygen (O) and fluorine (F) are the most frequent donor and acceptor atoms because of their high electronegativity.

All possible H-bond donors and acceptors in the simulation systems are evaluated for the existence of H-bonds in Gromacs. Two geometrical criteria are used to determine if an H-bond exists. According to the Figure 6, the criteria are: $\alpha \leq 30°$ and $r \leq 0.35\,nm$, where α is the Hydrogen-Donor-Acceptor angle and r is the Donor-Acceptor distance. Moreover, potential H-bonds are also recorded in Gromacs: the number of potential H-bonds is the number of H-bonds that could exists regarding only the criteria $r \leq 0.35\,nm$.

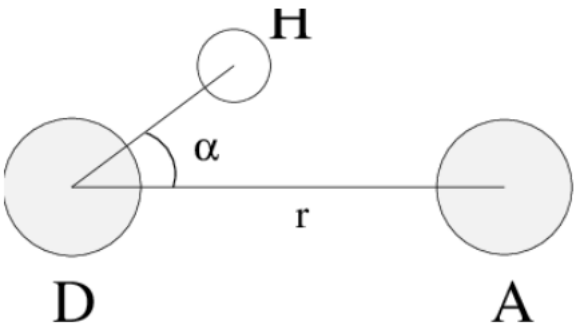

Figure 6 : Geometrical hydrogen bond criterion

As shown in Figure 7, the hydroxyl or hydroxy group is a functional group composed by one oxygen atom and one hydrogen atom. The term hydroxyl group refers more particularly to the hydroxy radical O-H, so to the unbonded hydroxy group. Hydroxy groups are likely to be engaged in hydrogen bonds because of the important difference of electronegativity between the oxygen atom and the hydrogen atom. Moreover hydroxy-containing compounds engaged in intermolecular H-bond increases the electrostatic attraction between molecules. An example of effect caused by the presence of hydroxy group is that organic molecules, often poorly soluble in water, become more soluble when they are composed of one or several hydroxy groups [13].

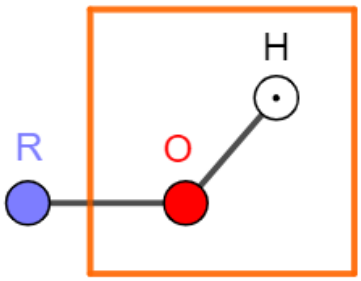

Figure 7 : Hydroxyl group or hydroxy group

1.2.3 Computing methods

In order to prepare equilibrated systems and accessing the role of hydroxyl groups in forming H-bonds, and further affect on the properties of MFP-like materials, different simulation techniques are used in this thesis. The following section provides a brief introduction of all the utilized methods.

To begin with, energy minimization (EM) is the most effective approach to achieve a spatial arrangement of a group of atoms with acceptable interatomic forces and potential energy [14]. EM is necessary to avoid MD simulation to fail because of a starting configuration including excessively large forces (two atoms too close from each other for example). Additionally, during this optimization certain coordinates, such as a chemical bond, are also optimized. Gromacs allows several algorithms to perform EM, the one we used in this study is the *steepest descent* method [15]. It is a reliable and robust method, easy to implement but it is not the most efficient. It calculates new coordinates following using the gradient of the forces or potential without consideration of the previous steps. The algorithm stops when the maximum absolute force is smaller than a required value or when the user-specified number of force evaluations has been realized.

Equilibration is the first simulating step coming after the EM. It includes specified pressure, temperature, velocities, and others similar components that were not taken into account during EM. The equilibration step allows the system to reach its stationary state. The molecules arrange themselves in a conformation similar to their experimental states. Different ensembles can be chosen for equilibration, for example two different ensembles are utilized in this work: the NPT ensemble where in the number of particles, pressure and temperature are all constant, and the NVT ensemble wherein the number of particles, volume and temperature are all constant. The first one will be particularly useful to simulate the system response to the external pressure to rearrange itself, avoiding small potential barriers and spatial bounding. Whereas with NVT equilibration the system relaxes in a given appropriated volume, with the possibility to include vacuum volume for interface effects, as naturally as possible.

Simulated annealing is a method to change the reference temperature of a part of the system or the whole system during a simulation. It models the physical process of heating a material and then slowly lowering the temperature to decrease defects, thus minimizing the system energy needed for effective conformation space sampling. The annealing is implemented by changing (not instantaneously) the current temperature of reference of the system or of a designed group of atoms. So, the actual relaxation and coupling properties depend on the number of thermostats used, the temperatures chosen, and the times chosen to reach these thermostats.

1.3 Molecular structure analyzis

There is already a good number of studies highlighting the importance of atomistic interactions to the properties of adhesive materials [16]. There is a known atomistic interaction type, namely the pi-interaction, that is crucial to the adhesive materials property [17]. The pi-interaction is a type of non-covalent interaction that involves a pi-system, which is in our study the benzene ring. Cation-π, anion-π and π-π interactions are three non-covalent bonds that are explained in previous studies [6]. In order to capture the pi-pi interaction in the simulation systems, the conformation of the benzene rings is thoroughly studied in this work. As indicated in previous studies [18], the π-π interaction between two aromatic species could be classified into three geometric categories (Figure 8): the edge-to-edge T-shape (preferred by the small unsubstituted aromatic compounds), the parallel-displaced geometry (preferred by substituted and large multiring aromatic compounds) and the cofacial or sandwich parallel stacked geometry (rather rarely observed). The benzene type of molecules has a quadrupole moment with partial negative electrostatic potential above both faces and a partial positive electrostatic potential around the periphery (Figure 9). Previous studies [17] indicates that two such quadrupole moments in proximity should prefer the edge-to-edge T-shape or parallel displaced geometry. A reversal of the polarization can occur if there are strong electron withdrawing groups attached to the aromatic ring. In that case the negative electrostatic potential is around the periphery and the positive electrostatic potential is above both the faces. Accordingly, if such electron-deficient quadrupole comes close to an electron-rich one, an electrostatic attraction takes place and the system adopt the cofacial parallel stacked geometry. Multiples studies have theoretically demonstrated that the T-shaped and parallel displaced geometries are stable and nearly isoenergetic whereas the cofacial parallel stacked geometry is least favoured in the case of benzene dimers [19].

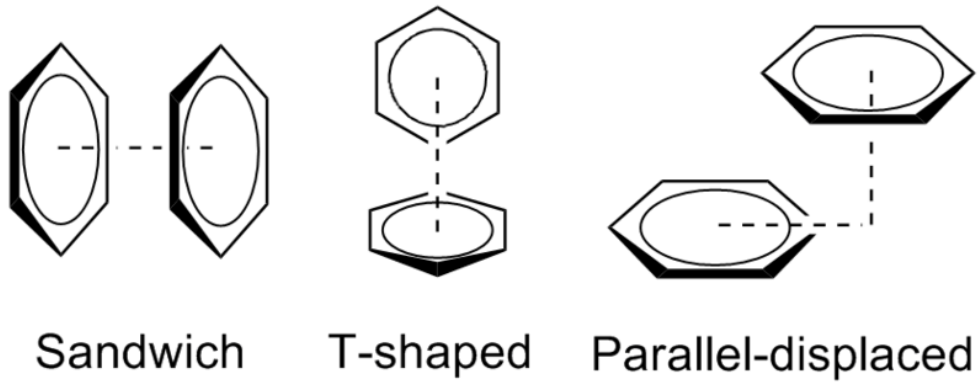

Figure 8 : π-π interaction conformations

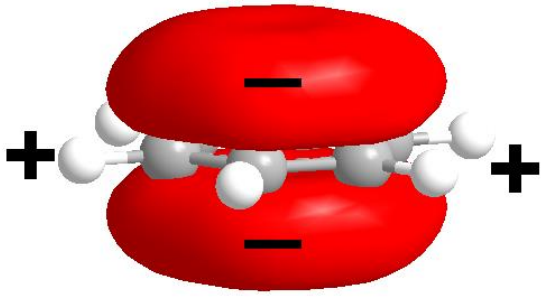

Figure 9 : Benzene quadrupole moment

In an important previous study [17], researchers introduced a model that indicates that the geometries of π-π interactions are controlled by electrostatic interactions but that the major energy contribution comes from other factors. According to their result, unfavourable contributions such as electron-π can be outdone by attractive contributions between π-electrons and the σ-framework. This is to what is due the π-π interactions and not an attractive electronic interaction. The model implies that the donor-acceptor concept can be misleading about the π-π interactions. The properties of the atoms in the region of the intermolecular contact control the interaction rather than the overall molecular potentials. Both of the so-called Atomic Charge Model and the Electron Donor-Acceptor Model were studied and rejected because they cannot explain or correspond with their experimental results. 3 rules for non-polarized π-systems were formulated to predict the most favourable geometry of interaction:

1. π-π repulsion dominates in a face-to-face π-stacked geometry.
2. π-σ attraction dominates in an edge-on or T-shaped geometry.
3. π-σ attraction dominates in an offset π-stacked geometry.

However, when the polarization effects are considered, the polarized pi-system follows extra rules:

4. For interactions between highly charged atoms, charge-charge interactions dominate.
5. A favourable interaction with a neutral or weakly polarized site requires the following π-polarization: (a) a π-deficient atom in a face-to-face geometry, (b) a π-deficient atom in a vertical T-group in the edge-on geometry, (c) a π-rich atom in the horizontal T-group in the edge-on geometry.

6. A favourable interaction with a neutral or weakly polarized site requires the following σ-polarization: (a) a positively charged atom in a face-to-face geometry, (b) a positively charged atom in the vertical T-group in the edge-on geometry, (c) a negatively charged atom in the horizontal T-group in the edge-on geometry.

According to this paper, the contribution of Van Der Waals interactions to the total energy will be proportional to the area of π-overlap and will vary with solvent as outlined above. In order to have a rough estimation of the magnitude of pi-interaction and the interaction geometric preferences, assumptions were adopted in previous studies [20]. Interaction between two benzenes rather than the whole phenylalanine monomers is used in the calculation. Moreover, the electrostatic potential around a benzene molecule has essentially radial symmetry, the interaction energy can be considered as independent of a third angle and studied with only two rotations. The Shortest Inter-Residue C-C Distance (SICD) was used as a criterion to decide if there is actually a π-π interaction or not: the criterion distance is 0,48 nm. The energy calculations were done by 3 methods. As such, the attractive and repulsive geometries depending on few parameters were obtained. Other studies has confirmed the above so-called Hunter-Sanders rules for non-polarized π-systems [20]. Finally, the previous study also indicated that π-π interactions between Phenylalanine residues in proteins occur predominantly in orientations that give rise to electrostatically favourable interactions, but that no single geometry correlates well with Hunter-Sanders rules for π-π interactions. In particular, offset stacked interactions are observed. Stacking with extensive π-overlap is believed to be unfavourable for non-polarized π-systems.

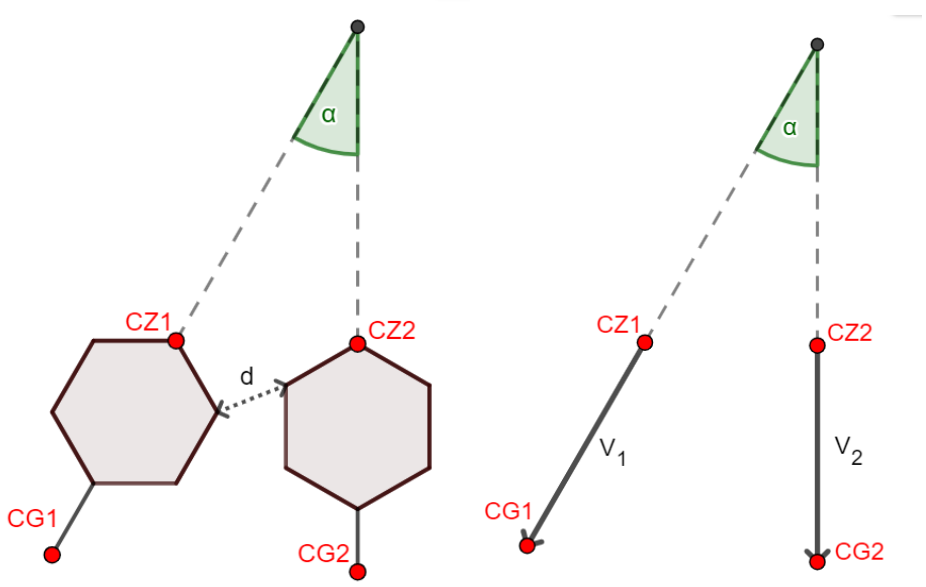

Figure 10 : Representation of the molecules, α and d in the Python code

Beside the simulations and analyses made with Gromacs in this study, Python was also used to analyze the final spatial configurations obtained with the simulations. According to the points made by the papers about π-conformation of benzene-containing molecules, we define an angle α and a SICD distance d for a given pair of molecules (see Figure 10). First the part of our molecules with the ring is represented as a vector, from the atom called CZ in the files to the atom called CG that links the benzene ring to the backbone. It must be noticed that this representation does not take in account the rotation of the benzene ring on the axis formed by these two atoms. α is the angle formed by the vectors symbolizing

the two molecules, and d is the shortest distance between two carbon atoms belonging to each ring. The values defined here are then used to detect the differences of the conformation among the molecules 0hydro to 3hydro. Thus, we will have an additional idea about the effect of the extra hydroxyl groups.

The same way [20] used the SICD and a cut-off distance to determine if there is interaction between two rings or not, a cut-off distance will be introduce in our code. The functioning of the python code applied to the simulation system is the following. Each molecule is assigned a distance from an atom in another molecule, and then the angle formed by the two molecules is calculated. It should be noted that often two molecules will be associated together twice in the process. For the molecules on the edge of the box, the calculation is made using the periodic boundary condition. Finally, the data on distances and associated angles will not be taken into account if $d > 0{,}48\ nm$. The value used for the cut-off agrees with the conclusion drawn following the approach in the previous studies [20] which is that a Phenylalanine-Phenylalanine interaction is judged to occur if the SICD is less than 0,48 nm.

2 Modeling and Simulation

2.1 Atomistic Parameterization

The goal of this work is to study the effect of varied number of hydroxyls on the properties of MFP-like materials through MD Simulation using the software Gromacs. Because such molecules are not provided by any standard force-field, the first step is to parameterize these molecules so that Gromacs can simulate them.

For each one of these four molecules, namely 0hydro, 1hydro, 2hydro and 3hydro with 0, 1, 2 and 3 hydroxyl group on the benzene ring in the sidechain of the monomers, two files named *conf.gro* and *topol.top* are prepared. The "gro" file extension contain a molecular structure in Gromos87 format, related to the software Gromacs. The second file is the topology file containing all the Gromacs specifications for an atomistic parameter (properties, kind of bonds and interactions, force fields, …). The main body structure of each of these two files are respectively given in Table 1 and Table 2 to facilitate the understanding of their content. Initially in this work the files corresponding to the molecules 0hydro and 1hydro were borrowed from amino acids of phenylalanine and tyrosine, respectively, with atomistic parameters from the OPLS force field [10]. So, additional hydroxyl group modification on the benzene ring was carried out taking 1hydro as template to keep the atomistic parameter format consistent, which result in two molecules of 2hydro and 3hydro.

Briefly, the procedure to create the new file *conf.gro* for 2hydro starting with a copy of the 1hydro's file is described here. Indeed, the molecule 1hydro already include a first hydroxy group and therefore its structure is closer than the 0hydro's structure to the one of the 2hydro. The modification consists in adding one oxygen atom between a carbon of the benzene ring and its hydrogen, in order to create a hydroxy group. As such, a new line was inserted for the new O atom between those corresponding to the two atoms C and H. In the new line:

- the residue number and name are the same as the carbon one line above with which the O is bonded (they are included in the same residue).
- an atom name is chosen and must be unique to this atom.
- the added oxygen atom takes the atom number of the hydrogen one line below with which the O is also bonded, and the atom numbers in all the following lines are shift by one.
- consistent coordinates are given regarding the length of a C-O bond, the position of the carbon atom and of the rest of the molecule. However, the hydrogen atom is now bonded to the added oxygen atom and no longer to the C atom. So, its position must also be modified regarding the length of a O-H bond, the position of the oxygen atom and of the rest of the molecule.

Following the formatting of *conf.gro* for 2hydro, the same protocol is followed to create the 3hydro *conf.gro* file, but this time starting with a copy of the file from 2hydro, including already two hydroxy groups.

The new file *topol.top* for 2hydro was created using 1hydro *topol.top* as a template. Specifically, a line is added between the concerned atoms C and H in the [atom] part of the file. As such, the [atom] part of the file is as follows:

- for each atom the "nr" must be the same as the atom number corresponding in *conf.gro.*
- In the column "types" we precise what OPLS will be used for the atoms, regarding to the atom and its environment. The added oxygen atom and its corresponding hydrogen have respectively the same types as the oxygen and hydrogen atoms of the first hydroxy group.
- The added oxygen's line takes the same "resnr" and residue as the carbon atom one line above, indicating that there are in the same structure.
- For each atom, the column "atom" must be fulfilled with the name used as atom name in *conf.gr*.
- The charges of the added oxygen and of the carbon and hydrogen atoms bonded to it must be modified with the same values as the atoms involved in the other hydroxy group.
- The "cgnr" refers to the groups of charge, each group of atoms has to be electrically neutral. In our case the new hydroxy group forms one electrically neutral group, so the three lines corresponding to the three atoms must have the same number in "cgnr".
- The mass of the new O is the same as the others oxygen atoms.

There is a [bonds] part in the file indicating all the covalent bonds in the molecule, each line precising the two atoms involved and the type of bond. The [pairs] part allows us to add extra Lennard-Jones or Coulombic interactions back between atoms by pairs. In the [angles] part is indicated how each angle formed by three bonded atoms in the molecule has to be treated about its vibration potential. Finally, the last part of the file is dedicated to proper and improper dihedrals, where all parameters defining dihedral (formed by four bonded atoms) planar, and how the angles and torsions energies among a dihedral are given.

Once again, the same protocol is applied to a copy of the final 2hydro *topol.top* in order to create the 3hydro *topol.top* file.

Title string				
Number of atoms				
Residue number	Residue name	Atom name	Atom number	Position (nm) (x,y,z)
…	…	…	…	…
…	…	…	…	…
Box vectors (Bx, By, Bz)				

Table 1 : Main body structure file .gro

[atoms]							
nr	type	resnr	residue	atom	cgnr	charge	mass
…	…	…	…	…	…	…	…
[bonds]							
ai	aj	funct					
…	…	…					
[pairs]							
ai	aj	funct					

…	…	…		
[angles]				
ai	aj	ak	funct	
…	…	…	…	
[dihedrals]				
ai	aj	ak	funct	Co
…	…	…	…	…

Table 2 : Main body structure file .top (ai, aj and ak are atoms numbers)

2.2 Bulk Study

Once the four molecules of this study are modeled for Gromacs, the role of hydroxy groups can be studied. In this first simulation part, the focus will be on the bulk properties of the materials. So, for each molecule the goal is to simulate a system filled with molecules in a state of equilibrium with minimum energy at a given temperature of $T = 300\,K$ and under the pressure of $P = 1\,bar$. In order to provide a statistical significance staying within achievable targets, three samples for each molecule type will be simulated. The protocol followed for each molecule type is described below.

Starting with the creation of the system, one square simulation box is created and filled with one thousand molecules like the one studied. The initial size of the box does not matter as long as the software succeeds in adding the 1000 molecules (Figure 11). Indeed, the box size will be adapted in the incoming simulation. An energy minimization (EM) is done with the steepest descent algorithm. The periodic boundary conditions are used for this simulation but also for all the following ones. So Gromacs will be able to calculate the potentials without crashing at the beginning of the next simulation, for example because of two molecules generated too close.

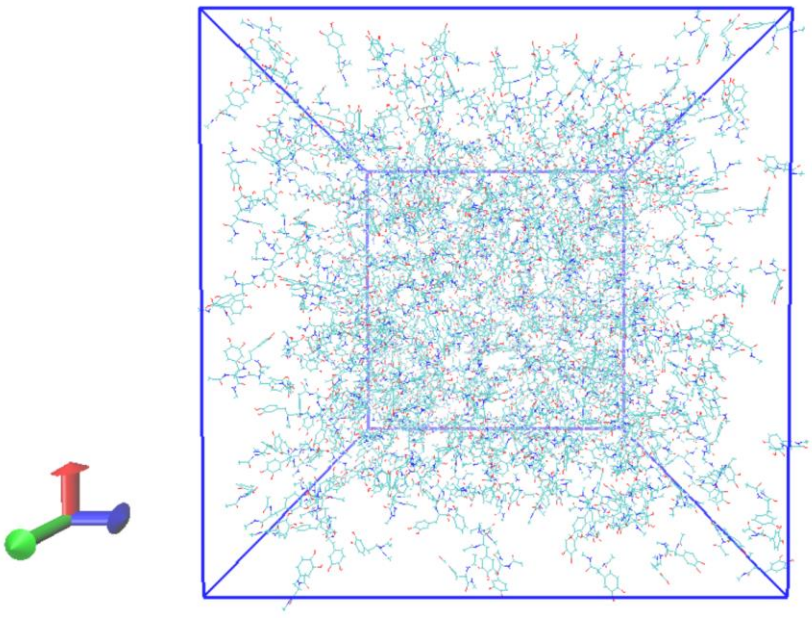

Figure 11 : Visualization in VDM of the box filled with 1000 2hydro molecules

Then an NPT equilibration is simulated during $t = 1\,ns$ ($dt = 0.002\,ps$, $nsteps = 500000$), using *md* (leap-frog algorithm for integrating Newton's equations of motion) as run control integrator. The *md* parameter will be used in all the simulation described below. The temperature is set at $T = 400\,K$ and the pressure is set at $P = 5\,bar$. The temperature and

pressure couplings are respectively done with the Nose-Hoover and Parrinello-Rahman algorithms [21]. A temperature higher than the final wanted temperature of 300 K is used to facilitate the movements of the molecules otherwise we obtain a bulk of material with void holes. Meanwhile a higher pressure must also be set to compensate for the increase in volume due to the higher temperature. This simulation is realized three times with three different random values of velocities among atoms in the systems, this way we obtain three different samples. Each sample starts this simulation with the same initial structure but evolves differently during the simulation. So, the final systems are independent. The simulations described below are done for each one of the three samples.

Another NPT equilibration is performed with the same algorithms but during $t = 10\,ns$ ($dt = 0.002\,ps$, $nsteps = 5000000$) at $T = 300\,K$ and $P = 1\,bar$. The system is well equilibrated, its potential energy is constant as is the box volume.

Finally a simulated annealing is performed with the following parameters: constant volume (same box dimensions as in the end of the last NPT equilibration), $t = 10\,ns$ ($dt = 0.002\,ps$, $nsteps = 5000000$), the temperature coupling is still done with the Nose-Hoover algorithm but 4 annealing points are specified for the temperature evolution as shown in Figure 12. Increasing the temperature allows the molecules to overcome energy barriers and then to a configuration, structure, thanks to a progressive cooling, with a lower potential energy. It must be noted that the system energies have been checked during the last 0,5 ns of the simulation (at the final target temperature) to make sure that 0,5 ns is enough for the system to equilibrate.

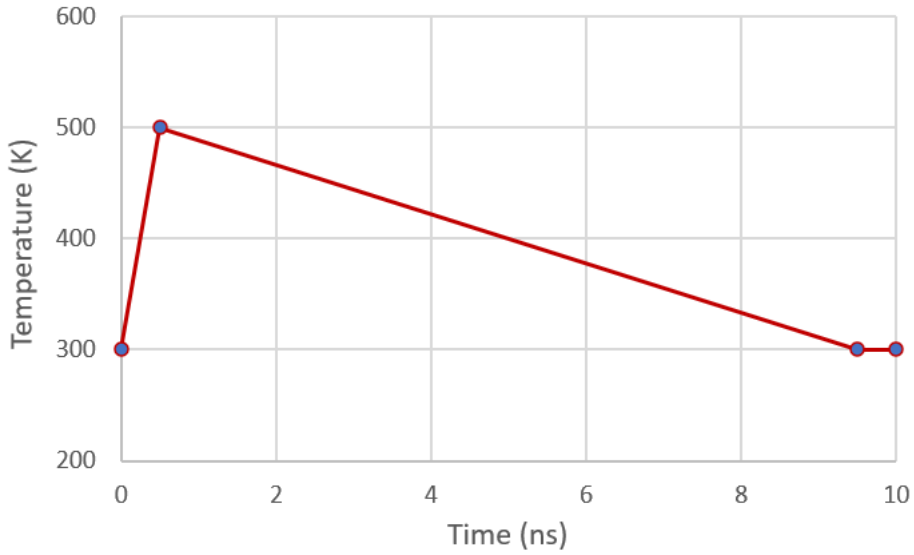

Figure 12 : Temperature evolution during the simulated annealing

The bulk obtained in the end of this simulated annealing is at equilibrium, at the target pressure and temperature, and still contains one thousand molecules. It can now be analyzed for a better understanding of the hydroxy group effects on the bulk properties of materials. The software Gromacs includes analysis packages. These functions directly give the system data over the duration of the simulation. Therefore, the numbers of hydrogen bonds and the energies within the system can be analyzed and comparisons between systems can be done. Moreover, an analysis of the final structure will be done using Python, in order to study the arrangement of the rings between themselves, using the parameters d and α described in the introduction of this work.

2.3 Layer Study

It is important to understand the adhesive properties of MFP-like materials at their interface, either toward the air or other materials. The Layer systems are prepared for such purpose. In the systems, vacuum buffer was created, which allows the molecules to organize and adapt to the vacuum space for the creation of a materials interface.

The model is realized from the bulk resulting from the last bulk simulation, the simulated annealing. Indeed, at this state the bulk is well equilibrated. The box y-dimension is extended to 15 nm i.e., about twice the side of the box. A layer as shown in Figure 13 is obtained.

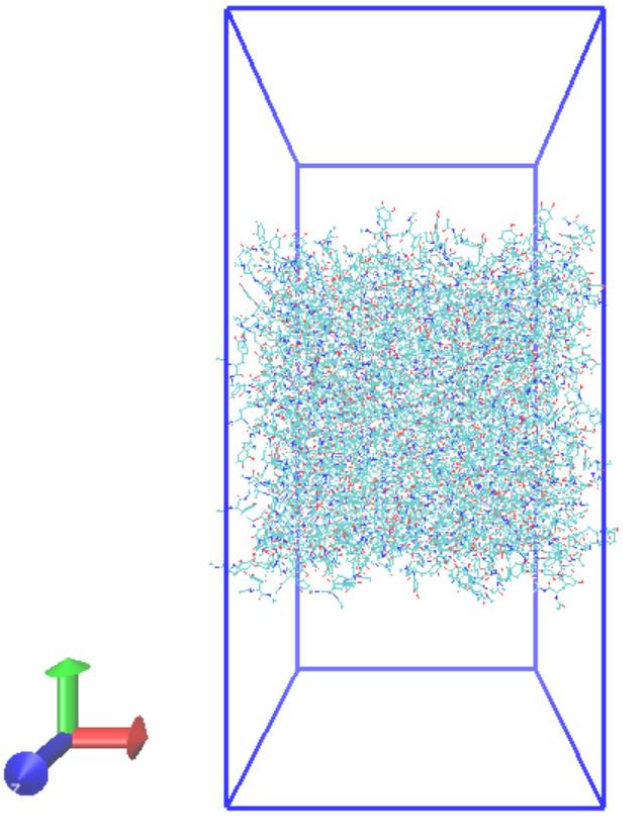

Figure 13 : Visualization in VMD of the layer box containing 1000 2hydro molecules

Because of the box dimension change, the molecules on the surface of the material are not at equilibrium anymore. A simulated annealing is performed with the same parameters as the simulated annealing done for the bulk and described above: $t = 10\,ns$ ($dt = 0.002\,ps$, $nsteps = 5000000$), at constant volume and still with the periodic boundary conditions, the temperature coupling is again done with the Nose-Hoover algorithm and 4 annealing points are specified for the temperature evolution as shown in Figure 12. The goal of this SA is to allows an important reorganization at the surface of the layer.

Then a NVT equilibration is simulated with the following parameters: $t = 10\,ns$ ($dt = 0.002\,ps$, $nsteps = 5000000$), constant volume and temperature $T = 300\,K$, Nose-Hoover algorithm for the temperature coupling, periodic boundary conditions. This step is to make sure the system has the time to equilibrate.

The final structure can now be analyzed for a better understanding of the hydroxy group effects on the layer properties of materials. The numbers of hydrogen bonds and the energies within the system can be analyzed and comparisons between systems can be done. Moreover, an analysis of the final structure will be done using Python, in order to study the arrangement of the rings between themselves.

2.4 Solvated Layer Study

A number of potential applications for the adhesive properties of derivatives of the DOPA molecule would be in contact with water. That is why the last system studied in this master thesis is a layer of material in contact with water on both sides.

The structure resulting from the layer study above is fulfilled with water as shown in Figure 14. Water molecules were introduced to fill the empty spaces i.e., above and below the layer, but also inside the layer between the 0hydro molecules.

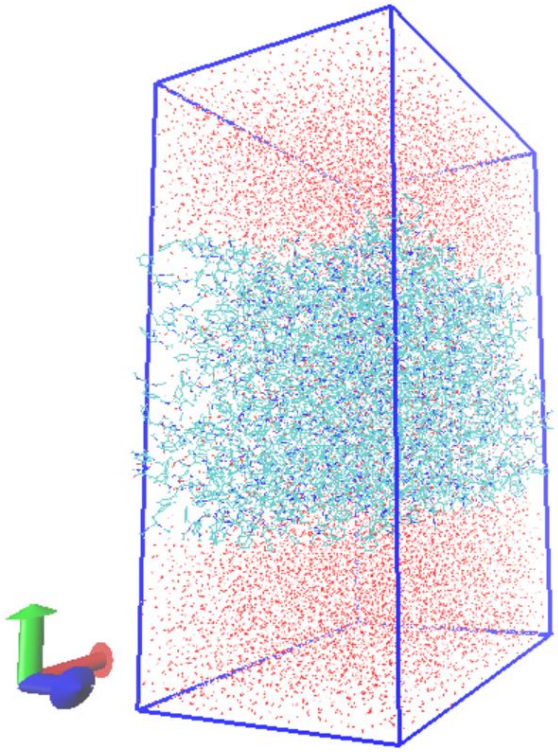

Figure 14: Visualization in VMD of the layer box containing 1000 0hydro molecules fulfilled with water molecules

The water molecules' introduction was made based on geometric considerations, so the whole process of equilibration must be done again. First an EM is performed with the steepest descent algorithm and the parameters ($dt = 0.001\,ps$, $nsteps = 10000$). We keep using the periodic boundary condition for those simulations as well as the Verlet cutoff-scheme.

Then a NPT equilibration is simulated during $t = 10\,ns$ ($dt = 0.002\,ps$, $nsteps = 5000000$), using *md* (leap-frog algorithm for integrating Newton's equations of motion) as run control integrator. The *md* parameter will be used in all the simulation described below. The temperature is set at $T = 300\,K$ and the pressure is set at $P = 1\,bar$. The temperature and pressure couplings are respectively done with the Nose-Hoover and Parrinello-Rahman algorithms. During this step the pressure is kept constant, but the volume can change when the box dimensions were kept constant since the NPT simulation for the bulk

structure. However, the temperature parameter is still the same so even with the added water molecules the box dimensions don't change significantly: the Table 3 gives one example of box dimensions change for each molecule type. The dimensions are almost the same before and after, as well as from one molecule to the next.

	0hydro Sample1	1hydro Sample1	2hydro Sample1	3hydro Sample1
Box Dimensions Before NPT	7.06720 15.00000 7.06720	7.17287 15.00000 7.17287	7.07332 15.00000 7.07332	7.14990 15.00000 7.14990
Box Dimensions After NPT	7.13212 15.13779 7.13212	7.22250 15.10379 7.22250	7.11909 15.09706 7.11909	7.19944 15.10393 7.19944

Table 3: Examples of box dimensions changes after the NPT simulation

The system is now equilibrated and is subjected to conformation space sampling to reorganize the internal molecular structures. A simulated annealing is performed with the following parameters: constant volume (same box dimensions as in the end of the last NPT equilibration), $t = 10\,ns$ ($dt = 0.002\,ps$, $nsteps = 5000000$), the temperature coupling is still done with the Nose-Hoover algorithm but 4 annealing points are specified for the temperature evolution as shown in Figure 12. Increasing the temperature allows the molecules to overcome energy barriers and then to a configuration, structure, thanks to a progressive cooling, with a lower potential energy. It allows more displacements in the system and the molecules structure fully takes in account the presence of the water molecules.

Then a NVT equilibration is simulated with the following parameters: $t = 10\,ns$ ($dt = 0.001\,ps$, $nsteps = 10000000$), constant volume and temperature $T = 300\,K$, Nose-Hoover algorithm for the temperature coupling, periodic boundary conditions. The time step parameter dt used is smaller than for all the other simulations to make sure that the water molecules displacements and vibrations are well simulated. This NVT makes sure the system has the time to equilibrate.

The solvated layer obtained in the end of this NVT equilibration is at equilibrium, at the target pressure and temperature. It can now be analyzed for a better understanding of the hydroxy group effects on the properties of materials as a layer in water. The analysis method is the same as for the bulk and the layer except that the hydrogen bonds analysis will be separated in two parts: hydrogen bonding among the DOPA derivatives, hydrogen bonding between DOPA derivatives and water. We may use *Xhydro* to designate the DOPA derivatives under study: 0hydro, 1hydro, 2hydro and 3hydro.

3 Results and Discussions

3.1 Atomistic parameterization and monomer minimization

The prepared molecular structures and the corresponding atomistic parameters need to be compatible with the required formats of the used simulation software Gromacs. Indeed, all the structures of the four monomers, namely 0hydro, 1hydro, 2hydro and 3hydro, were successful recognized by Gromacs. With the corresponding atomistic parameters, the four structures were first optimized by energy minimization to relax any internal stress in the molecular structure. As depicted by the optimized structured in Figure 15, all the four monomers gain the appropriate bond and angle values comparable with those provided in the OPLS force field [22]. However, this study aims at focusing on the catecholic sidechain properties. Therefore, two methyl groups were added to neutralize the terminals and reduce the interaction of the backbone.

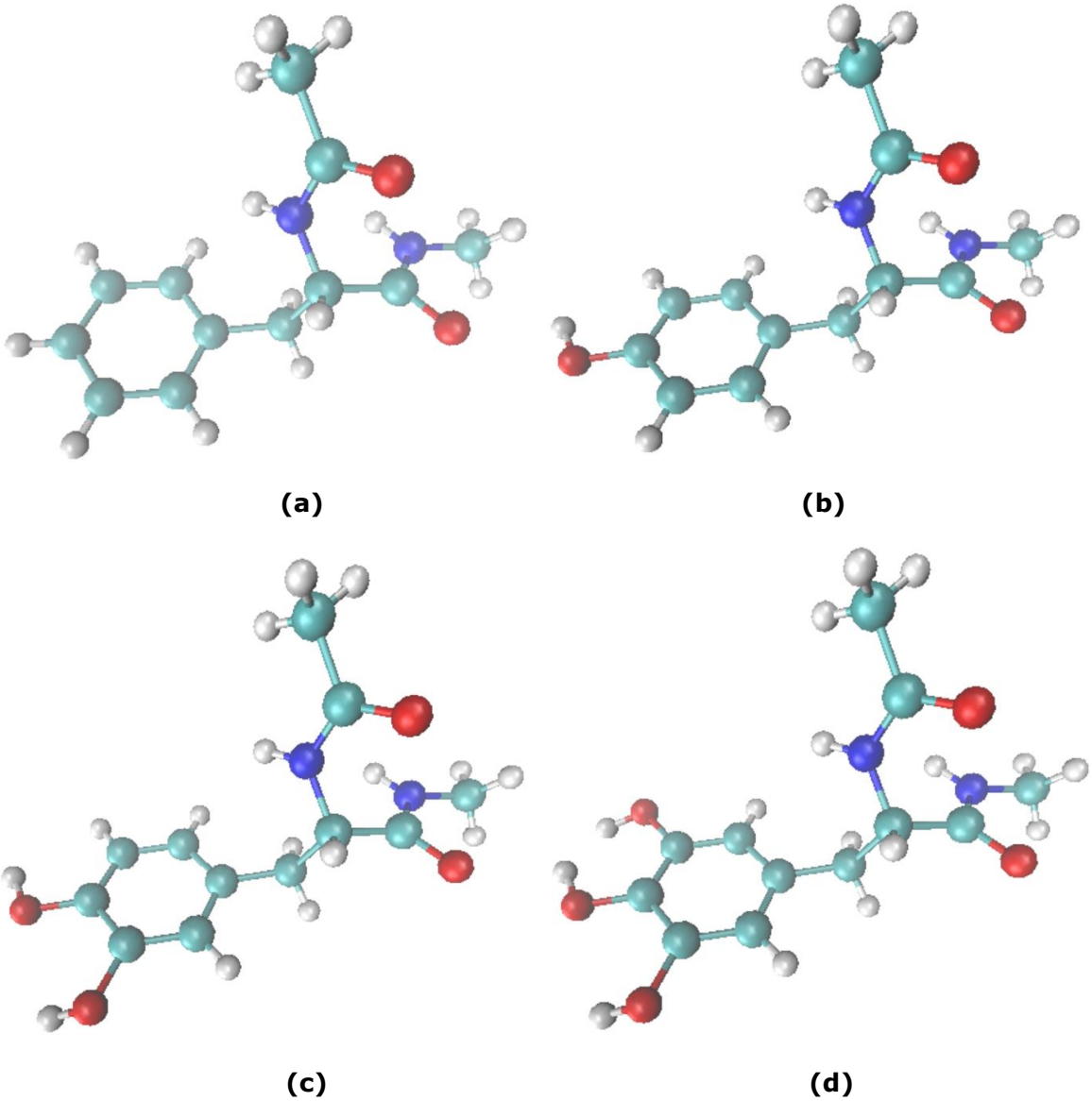

(a) **(b)**

(c) **(d)**

Figure 15 : (a) 0hydro. (b) 1hydro. (c) 2hydro. (d) 3hydro

3.2 Bulk study

As discussed in the Method section, the bulk materials of the four molecules are investigated by periodic simulation box with fully filled molecule. In such a setup, there is no interface in the system. Because simulated annealing enables the systems to explore a large conformational space of the system, the analysis in the follow section focuses only on the data obtained from simulated annealing simulation, if not otherwise specified. The results are presented and discussed in three topics, the hydrogen bonding, the energies and the structure arrangement.

3.2.1 Hydrogen-Bonds

The number of H-bonds in the system is monitored in the course of the simulated annealing simulation. As shown in Figure 16, the evolution of the number of H-bonds during the simulated annealing simulation. As expected it can be seen that the number of H-bonds decreases for each sample when the temperature increases, and on the contrary increases when the temperature decreases (the system stablelize itself creating H-bonds). Globally the differences between molecules are constant accross the simulation.

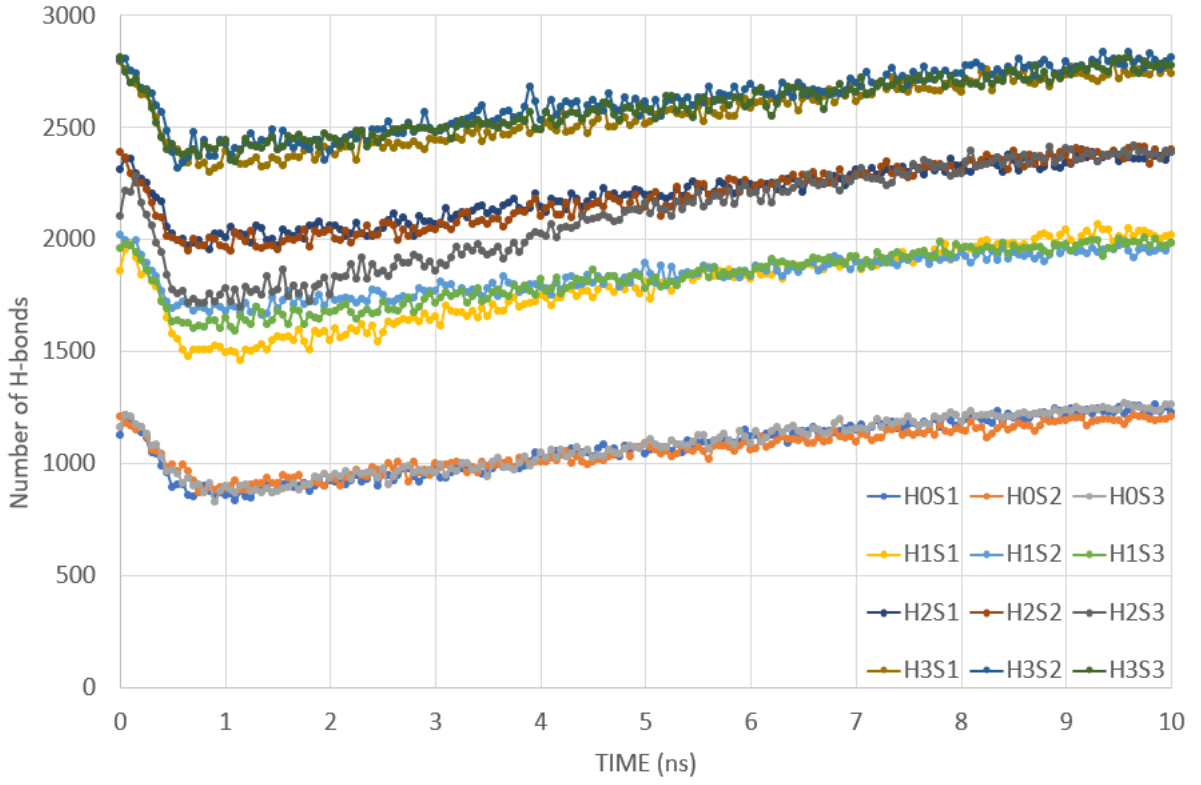

Figure 16 : Number of H-bonds evolution during simulated annealing for each sample

The different number of hydroxyl group of the four monomers indeed leads to varied number of H-bonds formed in the simulation systems. As shown in Figure 17, the mean number of H-bonds for each molecule, in the last part of the simulated annealing, when the system is at equilibrium. The number of H-bonds in the system increases with the number of hydroxy groups. As hydroxy groups are likely to be implied in a H-bond, the more hydroxy groups the system has, the more connections there are within the system. As expected, the hydroxyl groups in the systems actively participated in forming bonds.

The transition from 0 to 1 hydroxy group induces a bigger increase of the H-bonds number (+758 H-bonds) that the transition from 1hydro to 2hydro and from 2hydro to 3hydro (~400 H-bonds). The stable number of H-bonds in the end of the simulation is shown in Figure 17, the increase in H-bond number in 1hydro, 2hydro and 3hydro increases almost linearly. It should be noted here that 0hydro has no hydroxyl group on the benzene. All the H-bonds in the 0hydro system are by the backbone. As such, one extra hydroxyl group on the benzene ring could lead to the most abrupt increase in the number of H-bonds in the system. Further increase in the number of hydroxyl groups on the sidechain leads to almost constant increase in the overall number of H-bonds in the system. Thanks to the increased number of hydroxyl groups in the four systems from 0hydro to 3hydro, there is a corresponding increase trend hydrogen bond donors and acceptors in the four systems as shown in Appendix 1. Interestingly, the number of potential H-bonds increases less from 0hydro to 1hydro than for the others. The ratio number of new H-bonds divided number of new potential H-bonds is higher when the first group is added than for the following added hydroxyl groups.

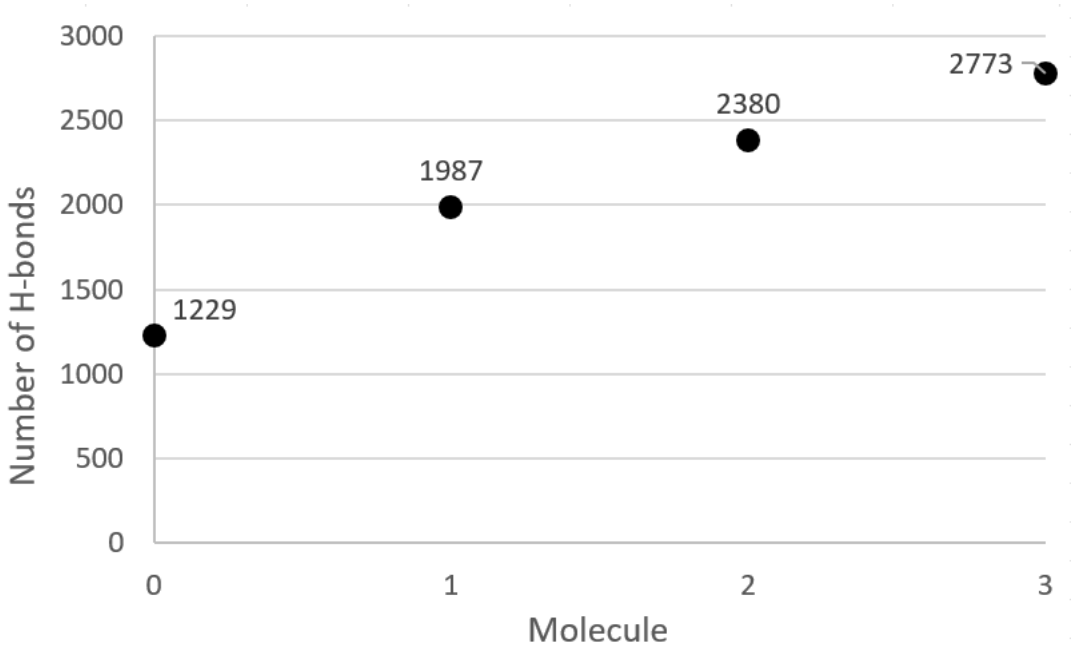

Figure 17 : Average number of H-bonds per molecule-type during the last 0,5 ns of the simulation

There is no obvious difference in H-bond angles among the four systems. As shown in Figure 18, all the H-bond angles fell in the range of 0 to 30 degree, with H-bond angle distribution in 3hydro slightly deviates from the other three systems. Such deviation is however negligible. Overall, the addition of hydroxyl group in the system did not alter the H-bond angles, despite the fact that H-bonds in the systems were formed from both the sidechain and the backbone.

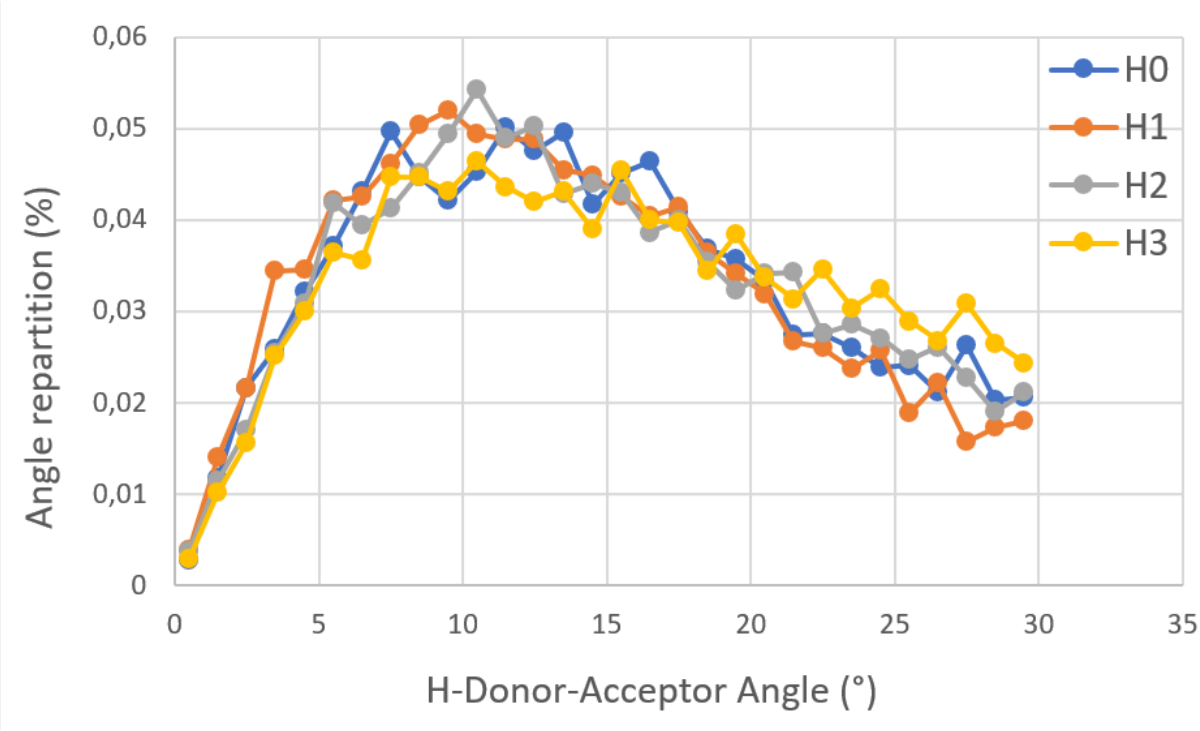

Figure 18 : Average repartition of the H-bond angle per molecule type

The same way the H-bond length repartition by molecule is given in Figure 19. There 0hydro distingishes itself very clearly meanwhile the other molecules curves are pretty much the same because hydrogen bonds in 0hydro are formed only by the backbone, the comparison of hydrogen bond distance between 0hydro with the other three system difference clear demonstrate the differences between hydrogen bonding by the sidechains and the backbone of the four modelled molecules. Hydroxyl groups on the sidechain, even only one, makes shorter hydrogen bonds in the systems. The shorter the bonds are, the stronger. So this result indicates that the 1hydro, 2hydro and 3hydro should have overall stronger internal molecular interactions, and thus higher cohesive energy than that of 0hydro.

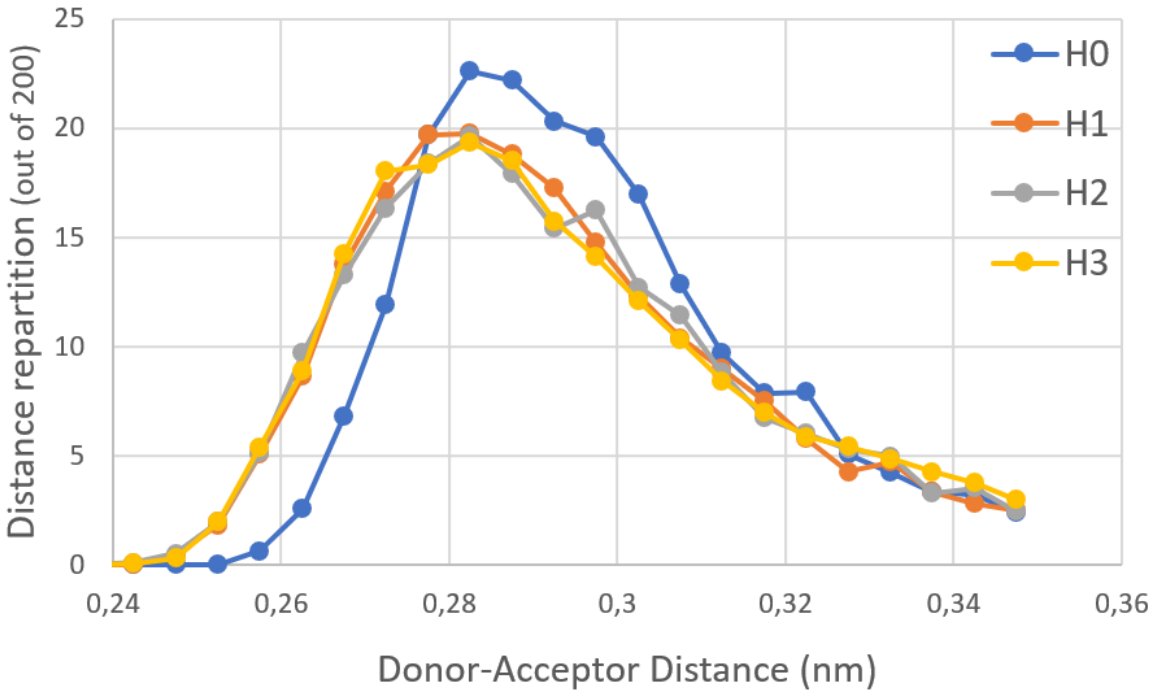

Figure 19 : Average repartition of the H-bond length per molecule type

In summary, the addition of hydroxy group in the system increases the number of H-bonds but also improves their strength. And the addition of the first group is definitely the one which affects the most the hydrogen bonds for the number of bonds and length. However, no conclusion can be made about the bond angles if not that the hydroxy groups have no sensible influence on it.

3.2.2 Energy

The system potential energy collectively summarized all the atomistic interactions in the system, which is an important quantity measuring the stability of the system. Furthermore, the items of the potential energy, namely the bond energy, the Lennard-Jones potential and the Coulombic potential gives more detailed information on their corresponding contribution to the overall system stability. The final system and the specific potentials after the simulated annealing are thus put together for comparison. For each molecule-type, the potential energy, the bond energy, the Lennard-Jones potential and the Coulombic potential are given respectively in Figure 20, Figure 21, Figure 22 and Figure 23. It's recalled here that the a system is composed of 1000 molecules, so dividing the energy or potential by 1000 gives directly the amount per molecule.

It can be seen in Figure 20 that the potential energy of the system decreases when the number of added hydroxy groups increases. The result was expected because of the increases of the number of hydrogen bonds found previously. Indeed the formation of hydrogen bonds leads to lower potential. The system is more stable with higher number of hydroxyl groups. However, it's noticeable that the decrease of the system potential energy of the system is irregular regarding the addition of hydroxy groups. The most important energy change is obtained by the transition from 1hydro to 2hydro.

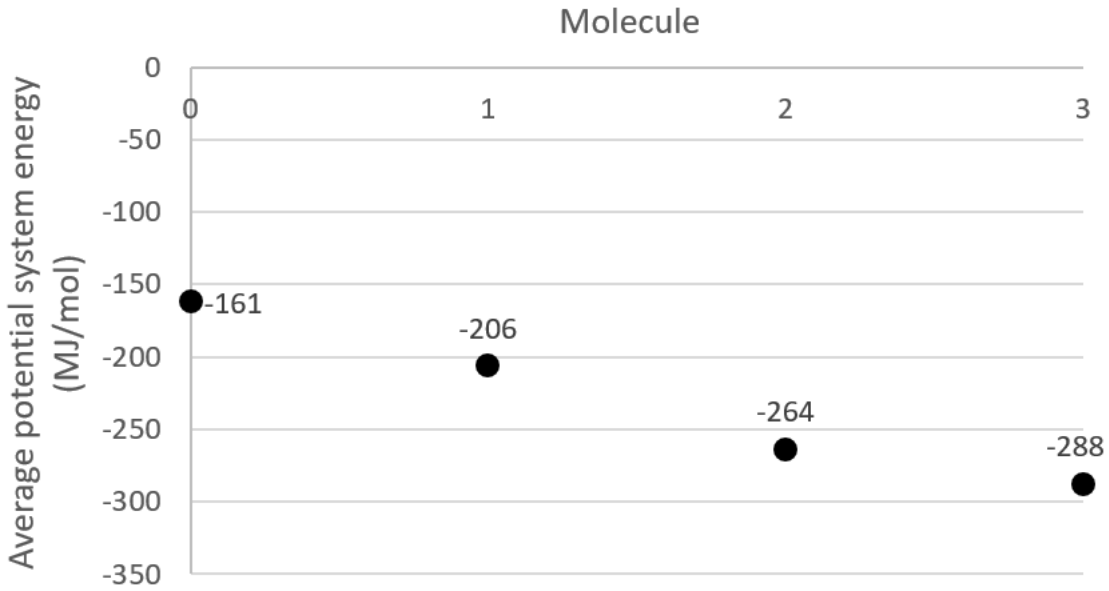

Figure 20 : Average potential system energy per molecule-type during the last 0,5 ns of the simulation

The bond energy shown Figure 21, called binding energy in physics and chemistry, represented the required energy to disassemble the system into individual parts. The higher is the number of bonds in the systems, the tighter the atoms are bonded and the system in general. Therefore the increase of the bond energy following the increase of the number of hydroxy groups makes perfectly sense. Meanwhile it can be observed that increases seems to be linear, mostly owing the linear increase in the number hydroxyl group in the four systems.

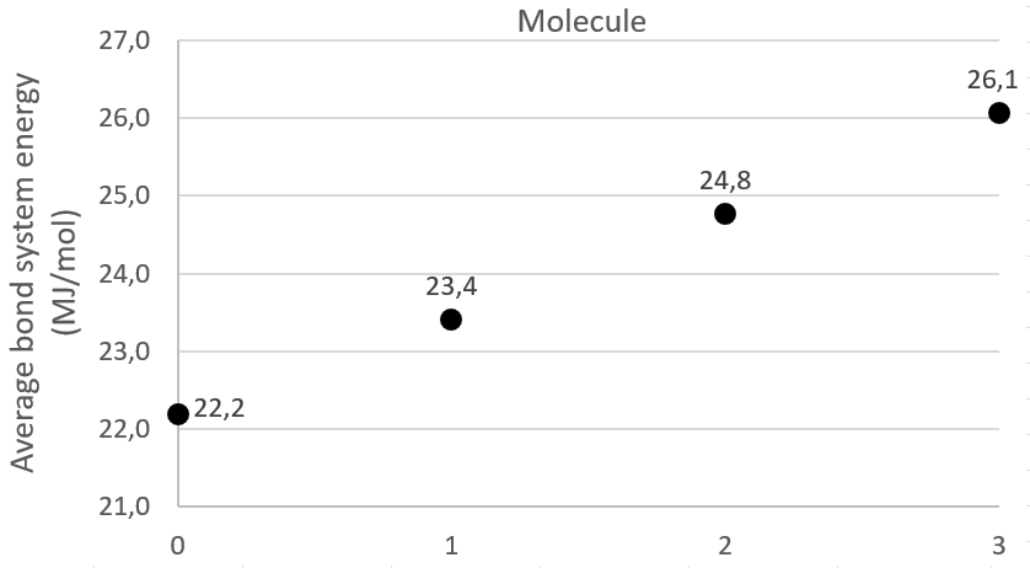

Figure 21 : Average bond system energy per molecule-type during the last 0,5 ns of the simulation

On the contrary, the evolutions of the Lennard-Jones and Coulombic potentials aren't consistent. It is important to note here that Lennard-Jones potential, together with Coulombic potential, is important to hydrogen bonding. The higher number of hydrogen bonds in the system, the lower Lennard-Jones potentials. Because the forming of hydrogen bonds is a random event in the simulation, deviation in the Lennard-Jones potential is thus

anticipated. Both decrease when the number of hydroxy groups increases because of the new interactions implied by the added electronegative oxygen atoms. The standard deviation is obvious in 1hydro, with 1 hydroxyl group in the sidechain. With increasing hydroxyl group in the sidechain, the deviation decreases and the Lennard-Jones potential decreases as well, showing the sidechains steadily form hydrogen bond with increasing number of hydrogen bonds in the system (Figure 22).

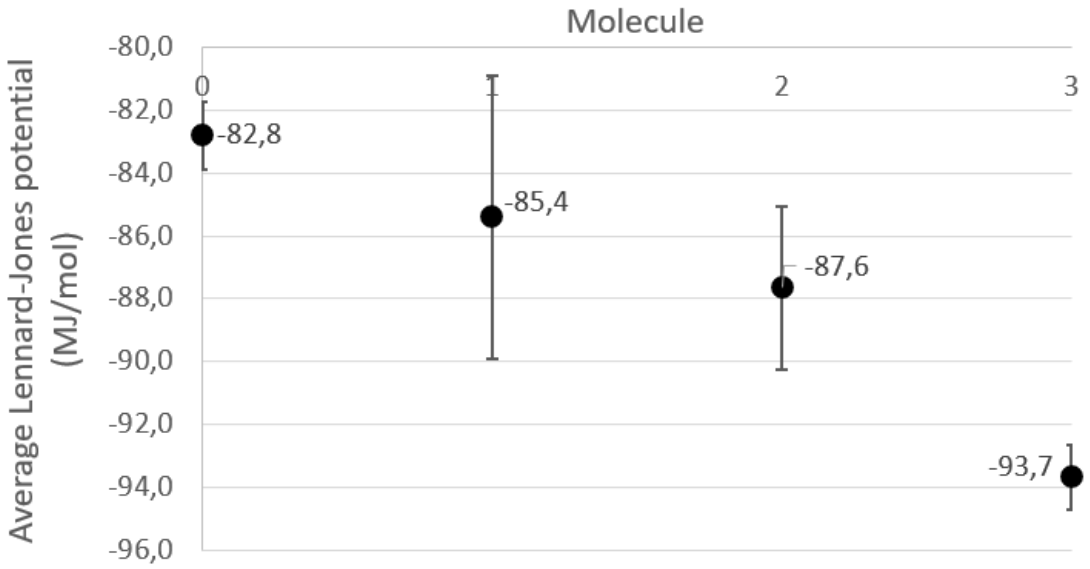

Figure 22 : Average system Lennard-Jones potential per molecule-type during the last 0,5 ns of the simulation. The error bars represent the average of the samples' standard deviation.

The Coulombic potential in the four system also shows a decreasing trend with increasing number of hydroxyl groups on the side-chain. Specifically, a small evolution is first observed (-16 MJ/mol from 0hydro to 1hydro) and then an important one (-215 MJ/mol from 1hydro to 2hydro). As such, it indicates that addition of two hydroxyl group in the sidechain could lead to an abrupt enhancement in the system Coulombic interactions, and thus the stability of the system.

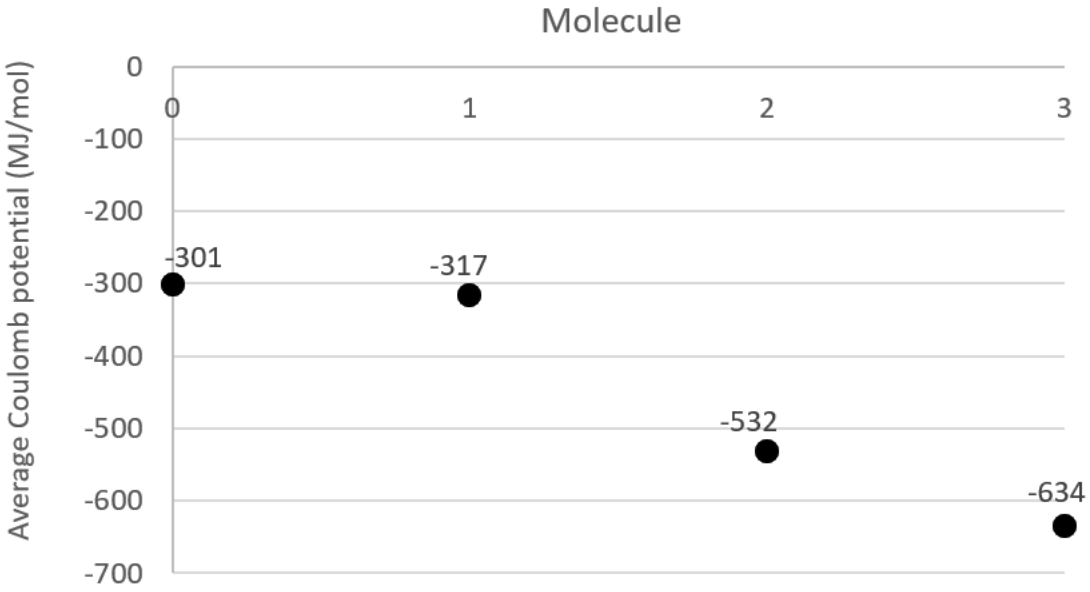

Figure 23: Average system Coulombic potential per molecule-type during the last 0,5 ns of the simulation

Finally, we can conclude that the adding hydroxy groups to the benzene ring of phenylalanine increases the system stability, namely by decreasing the overall system potential energy. The transition from 1hydro to 2hydro is particularly favorable to increase the Coulombic potential meanwhile the transition from 2hydro to 3hydro is more favorable to increase the Lennard-Jones interaction.

3.2.3 Python Code Analyzis

The organization of the molecules in the bulk system is analysed by the developed python codes in this work. So the parameters d and α described in 1.3 are used for the analyzis.

Table 4 presents the number of remaining values after the application of the cut-off. Between 100 and 150 values are deleted in each case, the vast majority of our rings are therefore considered to be interacting.

Molecule type	0hydro	1hydro	2hydro	3hydro
Number of remaining values d and α after the cut-off 0,48 nm	2897	2854	2854	2869

Table 4: Cut-off effect among the 3000 d and α calculated

Figure 24 shows for each molecule-type the distribution of angles for the π-π interactions detected in the final configuration of the system, after the simulated annealing. Besides, the average angles and standard deviations are gathered in Table 5. The average angle clearly increases from 0hydro to 1hydro, and then slowly decreases but not enough to be considered as a real change. However the standard deviation is important and it seems that there is not one strict favorable conformation. The average angle results confirm in a way the conclusion of [17] saying that the T-shape conformation ($\alpha \approx {}^{\pi}/_{2}$) is the most favorable arrangement for our molecules. Meanwhile it can be seen that for the molecules with added hydroxy groups, the probability density for high angles is higher than for 0hydro. It could be explained by the polarization of the ring by the oxygen atoms, which leads to more sandwich and parallel-displaced conformations in the bulk. Indeed [17]'s rule number 5 says that a π-deficient atom in a face-to-face geometry could lead to a favourable interaction with a neutral or weakly polarized site.

It is worth noting here that the shape of the distribution in Figure 24 also gives information of the effect of the number hydroxyl groups in the system. Specifically, the distribution of 0hydro features a normal distribution, while the distributions obtained from the other three systems show right-skewed shape. The addition of hydroxyl groups in the system clear affect the arrangement of the sidechains, and thus organization of the molecules.

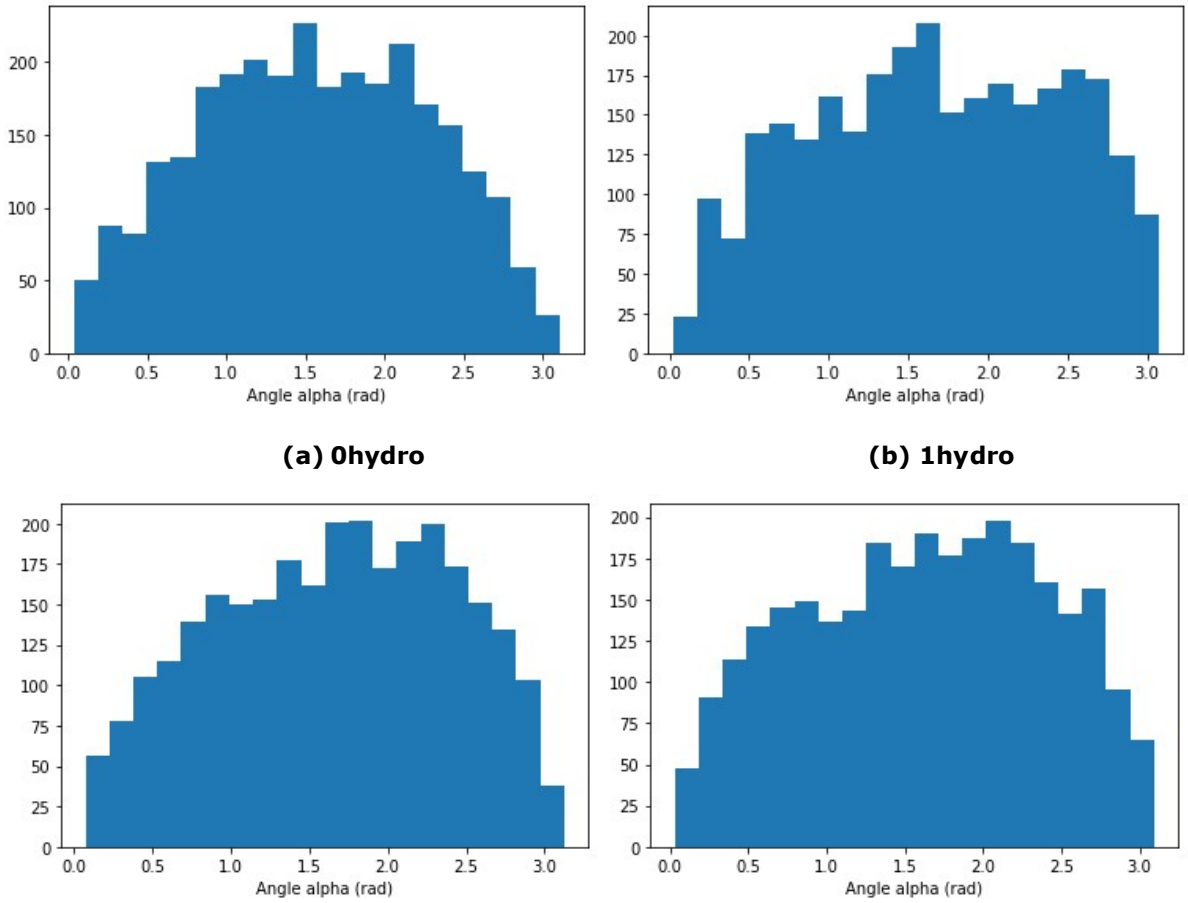

(a) 0hydro **(b) 1hydro**

(c) 2hydro **(d) 3hydro**

Figure 24 : Histogram of the angle α for each molecule, taking into account the 3 samples (i.e., 3000 angles calculated) and the cut-off

Molecule	0hydro	1hydro	2hydro	3hydro
α average (rad)	1,5582	1,6611	1,6585	1,6207
α standard deviation (rad)	0,7172	0,7745	0,7543	0,7710

Table 5 : α average and standard deviation values calculated with Python for each molecule, taking into account the 3 samples (i.e., 3000 angles calculated) and the cut-off

Then the Figure 25 demonstrates that the addition of the oxygen atoms to form hydroxy groups lenghtens the distance d between the rings. It can be explain by the fact that in the T-shape conformation for example, the oxygen is one more atom between the two carbons we use to calculate the inter-molecular distance d. The Table 6 makes clear the progressive increase of the distance d from 0hydro to 3hydro. The values are always between 0,3 nm and 4,8 nm. Previous studies [17] predict with the hard sphere atom model that the SICD must be between 0,34 and 4,8 nm for phenylalanine molecule. Our results are in line with this assumption, which confirms that they are within a relevant order of magnitude.

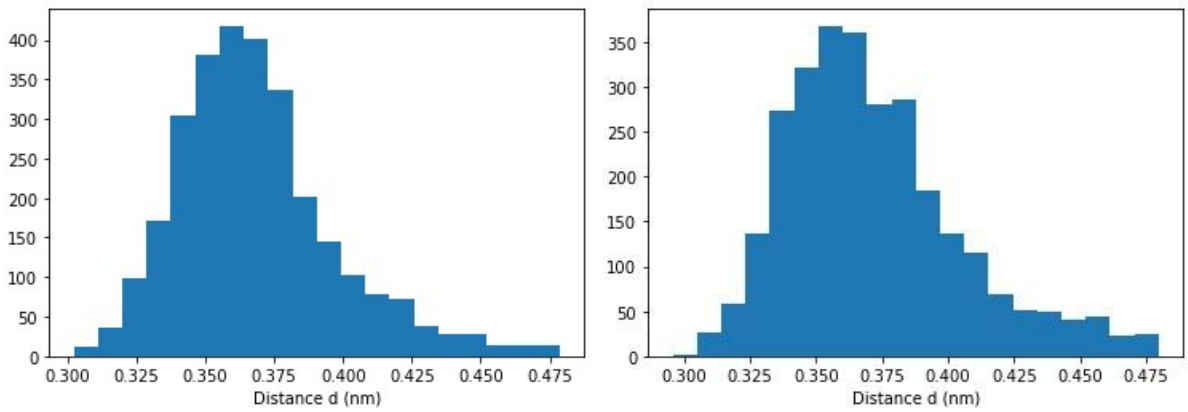

(a) 0hydro **(b) 1hydro**

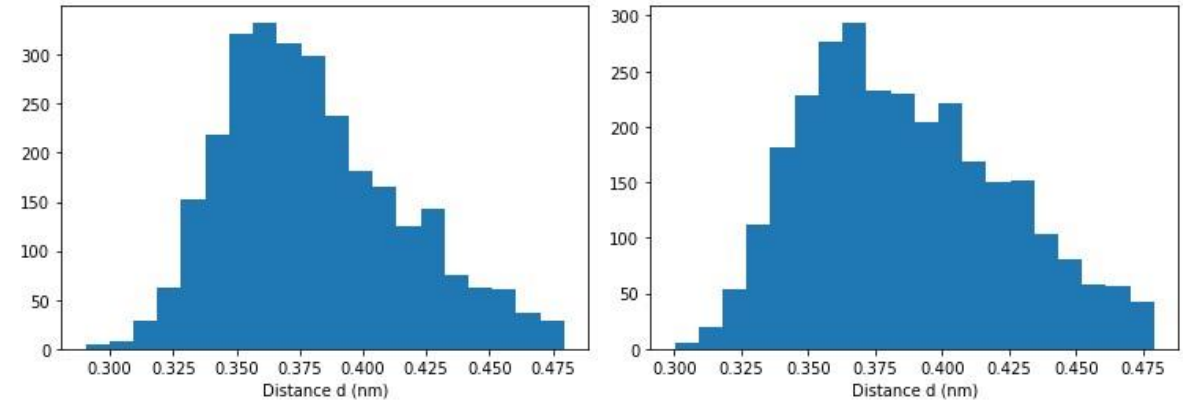

(c) 2hydro **(d) 3hydro**

Figure 25 : Histogram of the distance d for each molecule, taking into account the 3 samples (i.e., 3000 distances calculated) and the cut-off

Molecule	0hydro	1hydro	2hydro	3hydro
d average (nm)	0,3684	0,3718	0,3803	0,3862
d standard deviation (nm)	0,0290	0,0333	0,0351	0,0370

Table 6 : d average and standard deviation values calculated with Python for each molecule, taking into account the 3 samples (i.e., 3000 distances calculated) and the cut-off

So, the extra hydroxy groups result in a slight increase of the angle α even the distribution stay very similar, and in a gradual increase of the length d while maintaining the same value of maximum probability (~3,6 nm).

3.3 Layer Study

In this part, the results about the hydroxy groups influence on the layer properties are presented and discussed. The layer width is around 7 nm. The potential applications for an adhesive polymer and the boat hull coating improvement lead us to be interested more particularly in the behaviour of the material in surface. We indeed wonder if, comparatively to the bulk, the structure and intermolecular interactions change at the surface of the layer.

The analyze is divided the same way as it is for the bulk study, in three topics: the hydrogen bonds, the energies and the structure arrangement.

3.3.1 Hydrogen-Bonds

The number of the H-bonds in the systems are monitored in the course of the simulated annealing simulation. As shown in Figure 26, the evolution of the number of H-bonds during the NVT equilibration of the layer. As this simulation is an equilibration and the system was already somewhat in balance at the end of the previous simulated annealing, one can see that the numbers of H-bonds remains constant. However, as for the bulk, we notice that the differences between molecules are constant accross the simulation.

The different number of hydroxyl group of the four monomer indeed leads to varied number of H-bonds formed in the simulation systems. As shown in Figure 27, the mean number of H-bonds for each molecule, in the end of the NVT equilibration. The conclusion about the influence of the presence of hydroxy groups is exactly the same as for the bulk; indeed, with the final number of hydrogen bonds very close to that in the corresponding bulk systems (see Figure 17). The number of H-bonds in the system increases with the number of hydroxy groups. As the hydroxy groups are likely to be implied participating in a H-bond, the more hydroxy groups the system has, the more connections there are within the system. As expected, the hydroxyl groups in the systems actively participated in forming H-bonds. The transition from 0 to 1 hydroxy group induces a bigger increase of the H-bonds number (+739 H-bonds) that the transition from 1hydro to 2hydro and from 2hydro to 3hydro (~400 H-bonds). Thanks to the increase number of hydroxyl groups in the four systems from 0hydro to 3hydro, there are a corresponding increase trends hydrogen bond donors and accepter in the four systems, as shown by Appendix 2. Interestingly, the number of potential H-bonds increases less from 0hydro to 1hydro than for the others. The ratio number of new H-bonds divided number of new potential H-bonds is higher when the first group is added than for the following added hydroxyl groups.

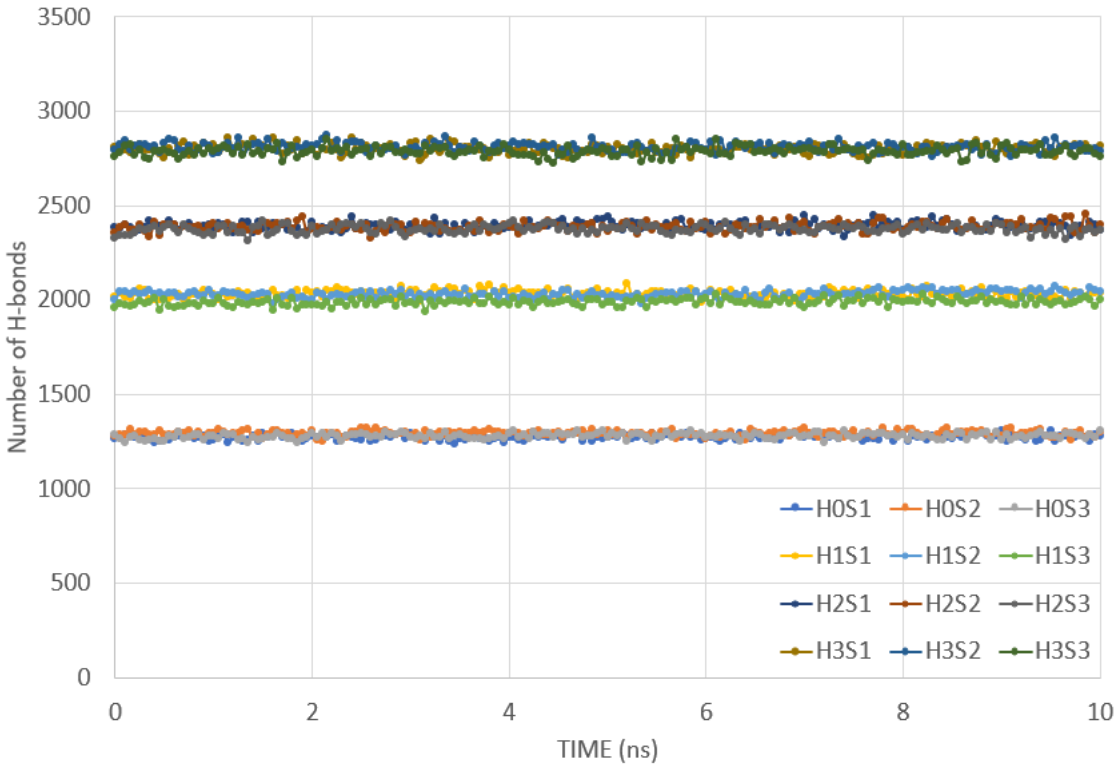

Figure 26 : Number of H-bonds evolution during NVT equilibration for each sample

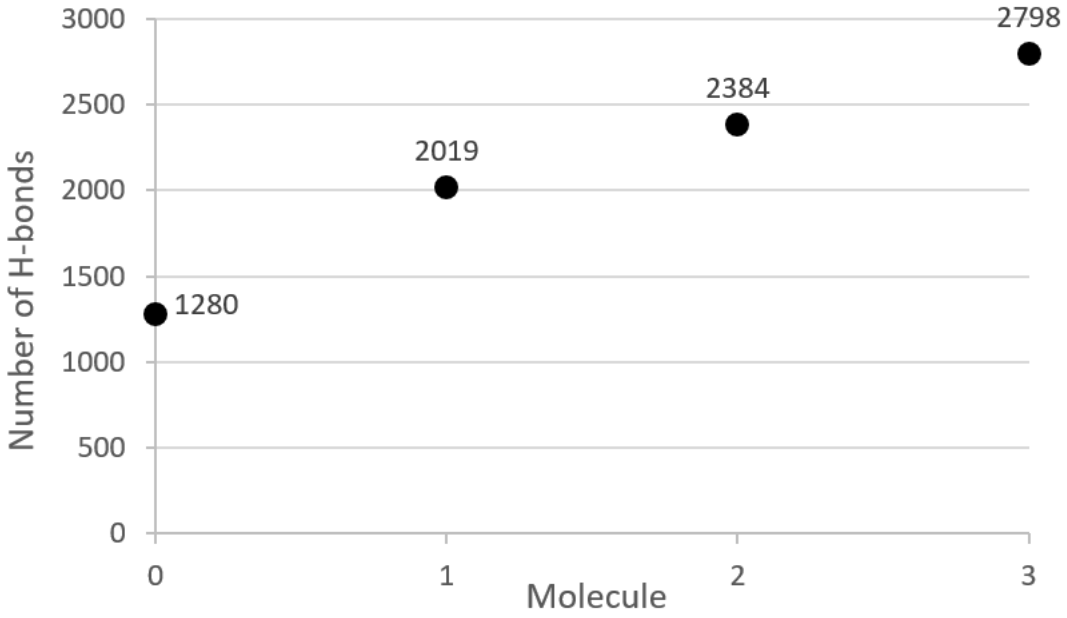

Figure 27 : Average number of H-bonds per molecule-type during the last 0,5 ns of the simulation

We find out that the number of H-bonds is slightly higher in the layer case. The opposite was expected because the molecules at the surface have fewer neighbors than in the bulk case and should be resulting in less bonds. That is first the sign that the simulated annealing and the equilibration worked well. Then it can be explained by the fact that the layer had a longer time to equilibrate and create H-bonds than the bulk had in the end of its simulated annealing.

There is no obvious difference in H-bond angles among the four systems. As shown in Figure 28, all the H-bond angles fell in the range of 0 to 30 degree, with H-bond angle distribution in 3hydro slightly deviates from the other three systems. Such deviation is however negligible. Overall, the addition of hydroxyl group in the system did not alter the H-bond angles, despite the fact that H-bonds in the systems were formed from both the sidechain and the backbone.

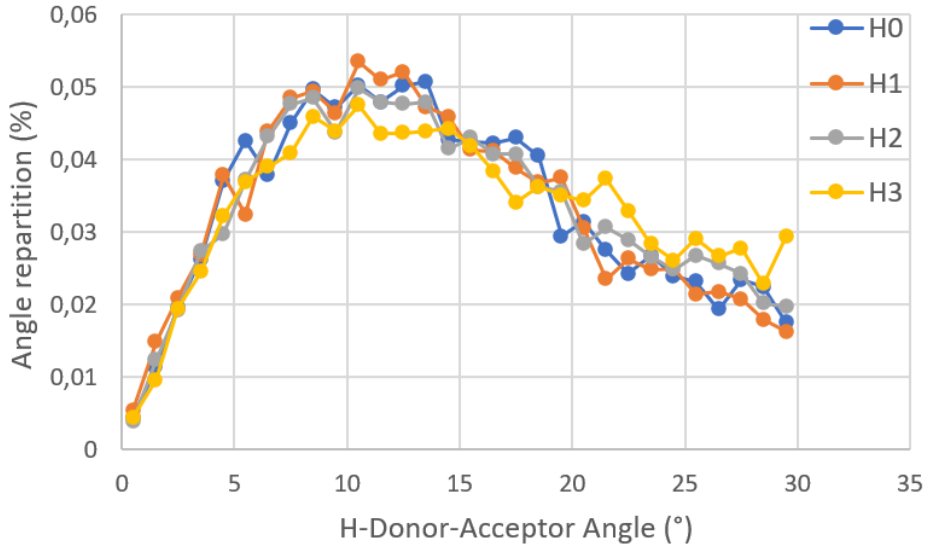

Figure 28 : Average repartition of the H-bond angle per molecule type

The same way the H-bond length repartition by molecule is given in Figure 29. The results indicates that 0hydro distingishes itself very clearly meanwhile the other molecules curves are pretty much the same. The addition of the hydroxyl groups on the sidechain, even only 1 in the 1hydro, makes shorter hydrogen bonds in the systems. The shorter the bonds are, the stronger. So this result indicates that the 1hydro, 2hydro and 3hydro should have overall stronger internal molecular interactionsn and thus higher cohesive energy than that of 0hydro.

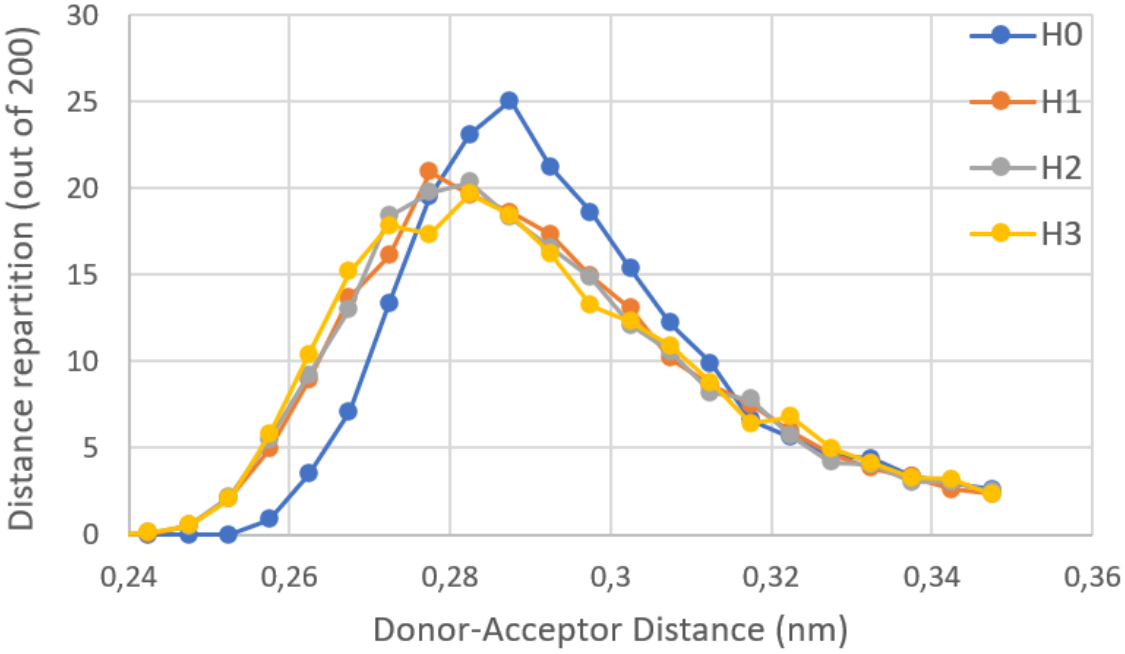

Figure 29 : Average repartition of the H-bond length per molecule type

In summary, the addition of hydroxy group in the system increases the number of H-bonds but also improves their strength. And the addition of the first group is the one which affects the most the hydrogen bonds for the number of bonds and length. However, no conclusion can be made about the bond angles if not that the hydroxy groups have no sensible influence on it.

Moreover, this first part allows us to conclude that the hydrogen bonding works the same in the layer and bulk structures.

3.3.2 Energy

As discussed above, the energetic properties of the system is an good indication of the system stability, which are also analysed for the layer systems. For each molecule-type, the potential energy, the bond energy, the Lennard-Jones potential and the Coulombic potential are given respectively in Figure 30, Figure 31, Figure 32 and Figure 33. It's recalled here that the a system is composed of one thousand molecules, so dividing the energy or potential by one thousand gives directly the amount per molecule.

It can be seen in Figure 30 that the potential energy of the system decreases when the number of added hydroxy groups increases. The result was expected because of the increases of the number of hydrogen bonds found previously. Indeed the formation of hydrogen bonds leads to lower potential. The system is more stable with higher number of hydroxyl groups. However, it's noticeable that the decrease of the system potential energy

of the system is irregular regarding the addition of hydroxy groups. The most important energy change is obtained by the transition from 1hydro to 2hydro.

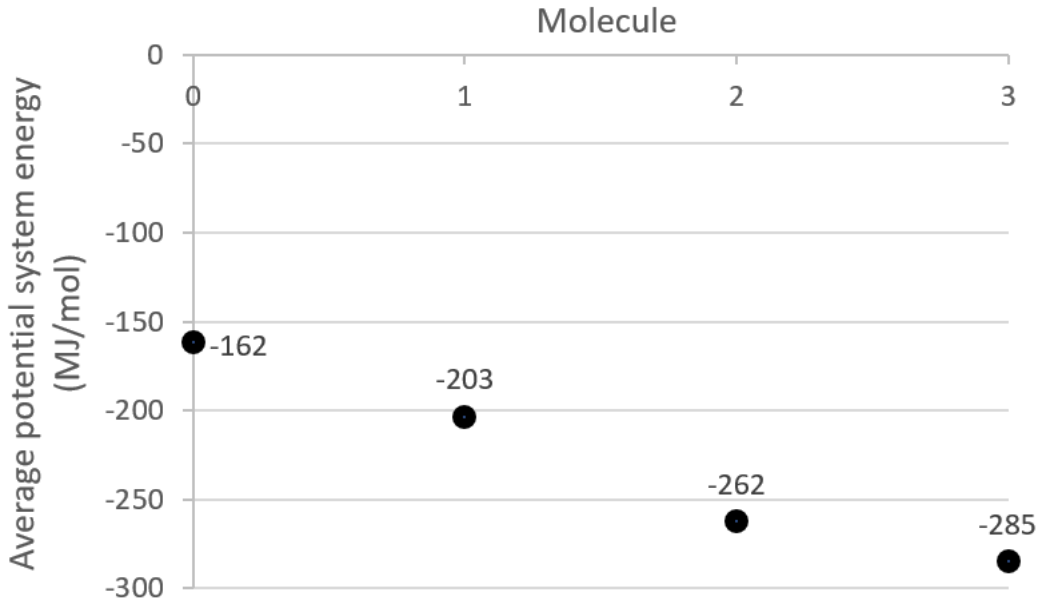

Figure 30 : Average potential system energy per molecule-type during the last 0,5 ns of the simulation

The bond energy shown Figure 31, called binding energy in physics and chemistry, represented the required energy to disassemble the system into individual parts. The higher is number of bonds in the systems, the tighter the atoms are bonded and the system in general. Therefore the increase of the bond energy following the increase of the number of hydroxy groups makes perfectly sense. Meanwhile it can be observed that increases seems to be linear, mostly owing the linear increase in the number hydroxyl group in the four systems.

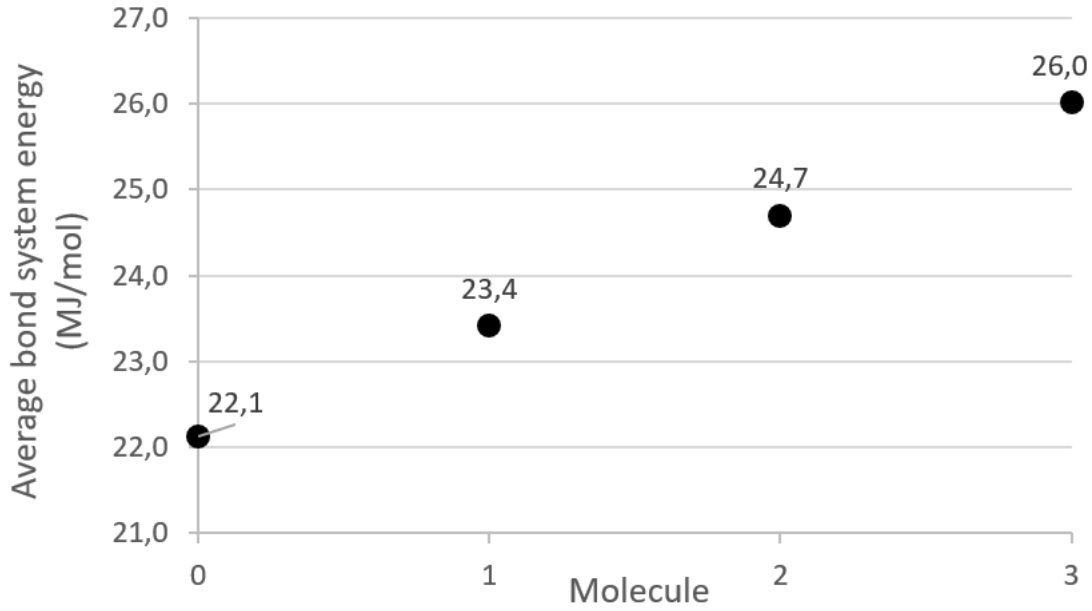

Figure 31 : Average bond system energy per molecule-type during the last 0,5 ns of the simulation

On the contrary, the evolutions of the Lennard-Jones and Coulombic potentials aren't consistent. Both decrease when the number of hydroxy groups increases because of the new interactions implied by the added electronegative oxygen atoms. The standard deviation is relevant to be shown for the Lennard-Jones potential, however they're too small to be represented on the other figures. The comparison of the error bars with those from the Figure 22 shows that the results are more regular in the layer configuration. This may be because of the longer equilibration of the system. These values indicate that the transition from 1hydro to 2hydro and from 2hydro to 3hydro have a bigger impact on the Lennard-Jones interaction.

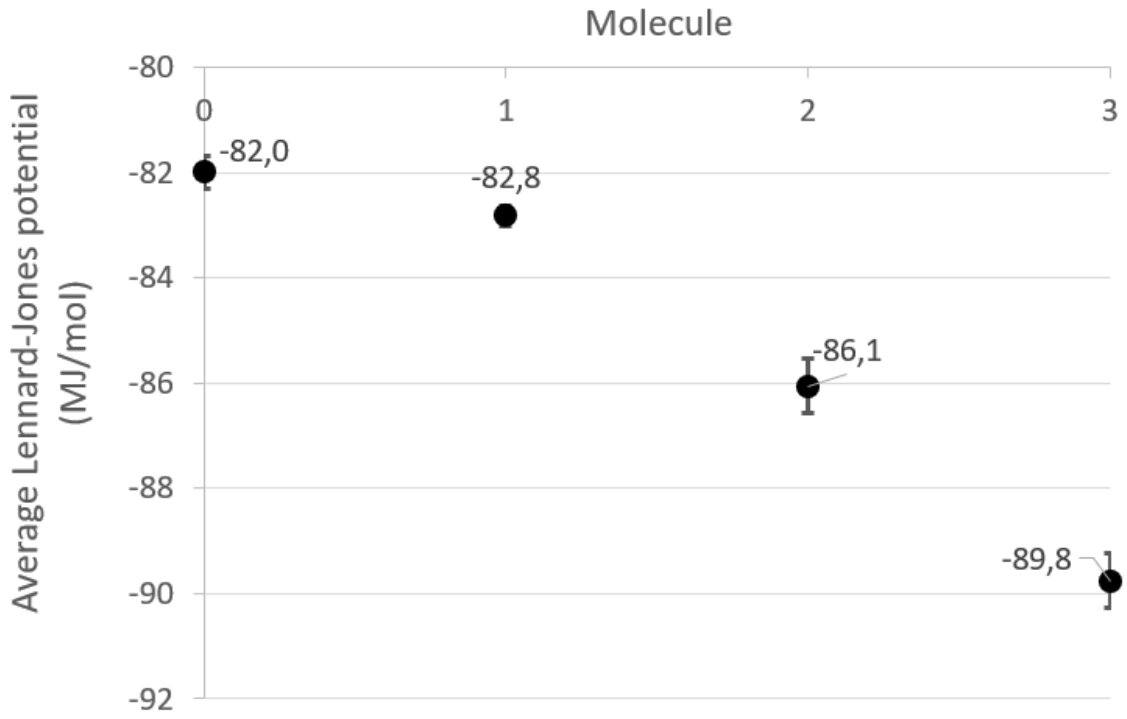

Figure 32 : Average system Lennard-Jones potential per molecule-type during the last 0,5 ns of the simulation. The error bars represent the average of the sample's standard deviation

The Coulombic potential in the four system also shows a decreasing trend with increasing number of hydroxyl groups on the side-chain (Figure 33). Specifically, a small evolution is first observed (-16 MJ/mol from 0hydro to 1hydro) and then an important one (-216 MJ/mol from 1hydro to 2hydro). It has the same phenomenon as what observed in the bulk system. Two additional hydroxyl groups leads to abrupt enhancement of coulombic interaction in the system. As such, the result is also in accord with the enhanced adhesive properties of DOPA, having two hydroxyl groups, if compared with tyrosine [23]. This interesting effect is worth further investigating in the future study.

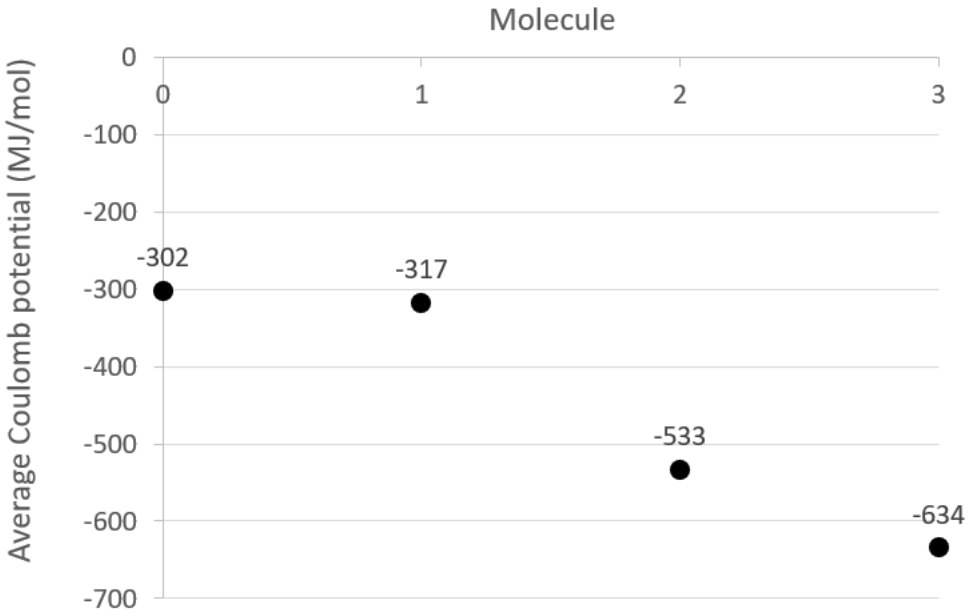

Figure 33 : Average system Coulombic potential per molecule-type during the last 0,5 ns of the simulation

Finally, we can conclude that the adding hydroxy groups to the benzene ring of phenylalanine increases the system stability, namely by decreasing the overall of the system potential energy. The transition from 1hydro to 2hydro is particularly favorable to increase the Coulombic potential meanwhile the transition from 2hydro to 3hydro is more favorable to increase the Lennard-Jones interaction.

If we compare the energy results with those from the bulk configuration, we can see that the values always are pretty close. However, the results seem more precise in the layer configuration thanks to an additional equilibration after the simulated annealing. Besides, the values of energy interaction are slightly smaller in the layer configuration; the fewer interaction opportunities for the molecules in the surface may decrease the global energies of interaction, even though we saw previously that the layer configuration contains more H-bonds.

3.3.3 Python Code Analysis

The organization of the molecules in the bulk system is analysed by the developed Python codes in this work. So the parameters d and α described in Introduction are used for the analyzis.

Table 7 presents the number of remaining values after the application of the cut-off. Between 100 and 150 values are deleted in each case, the vast majority of our rings are therefore considered to be interacting.

Molecule type	0hydro	1hydro	2hydro	3hydro
Number of remaining values d and α after the cut-off 0,48 nm	2898	2890	2893	2890

Table 7 : Cut-off effect among the 3000 d and α calculated

Figure 34 shows for each molecule-type the distribution of the angles for the π-π interactions detected in the final configuration of the system, after the simulated annealing.

Besides, the average angles and standard deviations are gathered in Table 8. The standard deviation is important and it seems that there is not one strict favorable conformation. The average angle results confirms in a way the conclusion of [17] saying that the T-shape conformation ($\alpha \approx {}^{\pi}/_{2}$) could be the most favorable arrangement for our molecules. Meanwhile it can be seen that for the molecules with added hydroxy groups, the probability density for high angles is higher than for 0hydro, particularly in the case of 1hydro for which the average α reaches 1,6716 rad. It could be explained by the polarization of the ring by the oxygen atoms, which leads to more sandwich and parallel-displaced conformations in the bulk. Indeed previous studies' [17] rule number 5 says that a π-deficient atom in a face-to-face geometry could lead to a favourable interaction with a neutral or weakly polarized site.

In the layer configuration the main change may be from the transition from 0hydro to 1hydro meanwhile the next additions are steps backwards. We notice that in this case the value with the maximum probability to occur is between 2 and 2,5 rad for 1hydro, 2hydro and 3hydro.

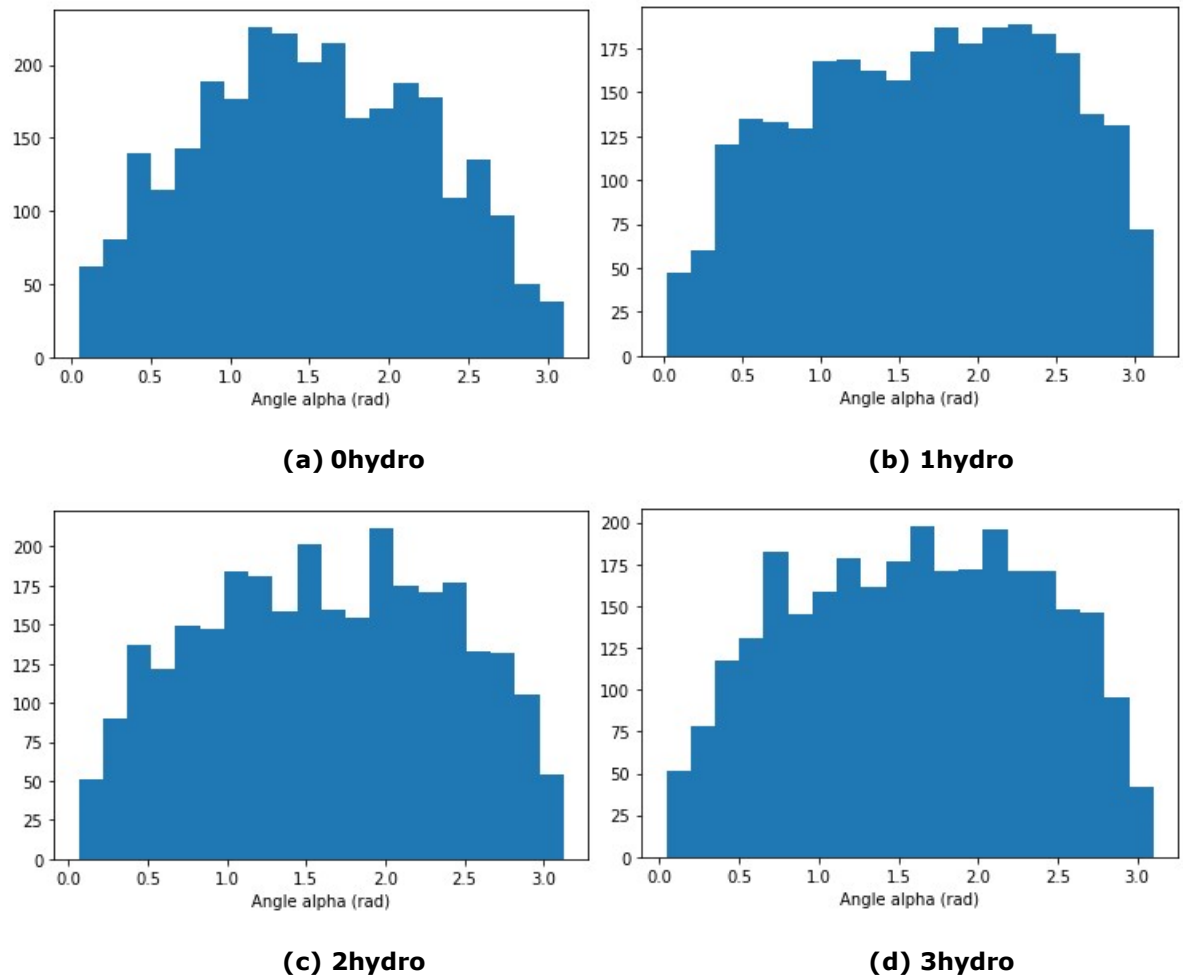

(a) 0hydro **(b) 1hydro**

(c) 2hydro **(d) 3hydro**

Figure 34 : Histogram of the angle α for each molecule, taking into account the 3 samples (i.e., 3000 angles calculated) and the cut-off

Molecule	0hydro	1hydro	2hydro	3hydro
α average (rad)	1,5160	1,6716	1,6202	1,6036

α standard deviation (rad)	0,7225	0,7870	0,7704	0,7630

Table 8 : α average and standard deviation values calculated with Python for each molecule, taking into account the 3 samples (i.e., 3000 angles calculated) and the cut-off

As for the bulk configuration, the Figure 35 demonstrates that the addition of the oxygen atoms to form hydroxy groups lenghtens the distance d between the rings. It can be explain by the fact that in the T-shape conformation for example, the oxygen is one more atom between the two carbons we use to calculate the inter-molecular distance d, but also by the change of the molecule's moment. Table 9 makes clear the progressive increase of the distance d with the additions of hydroxy group.

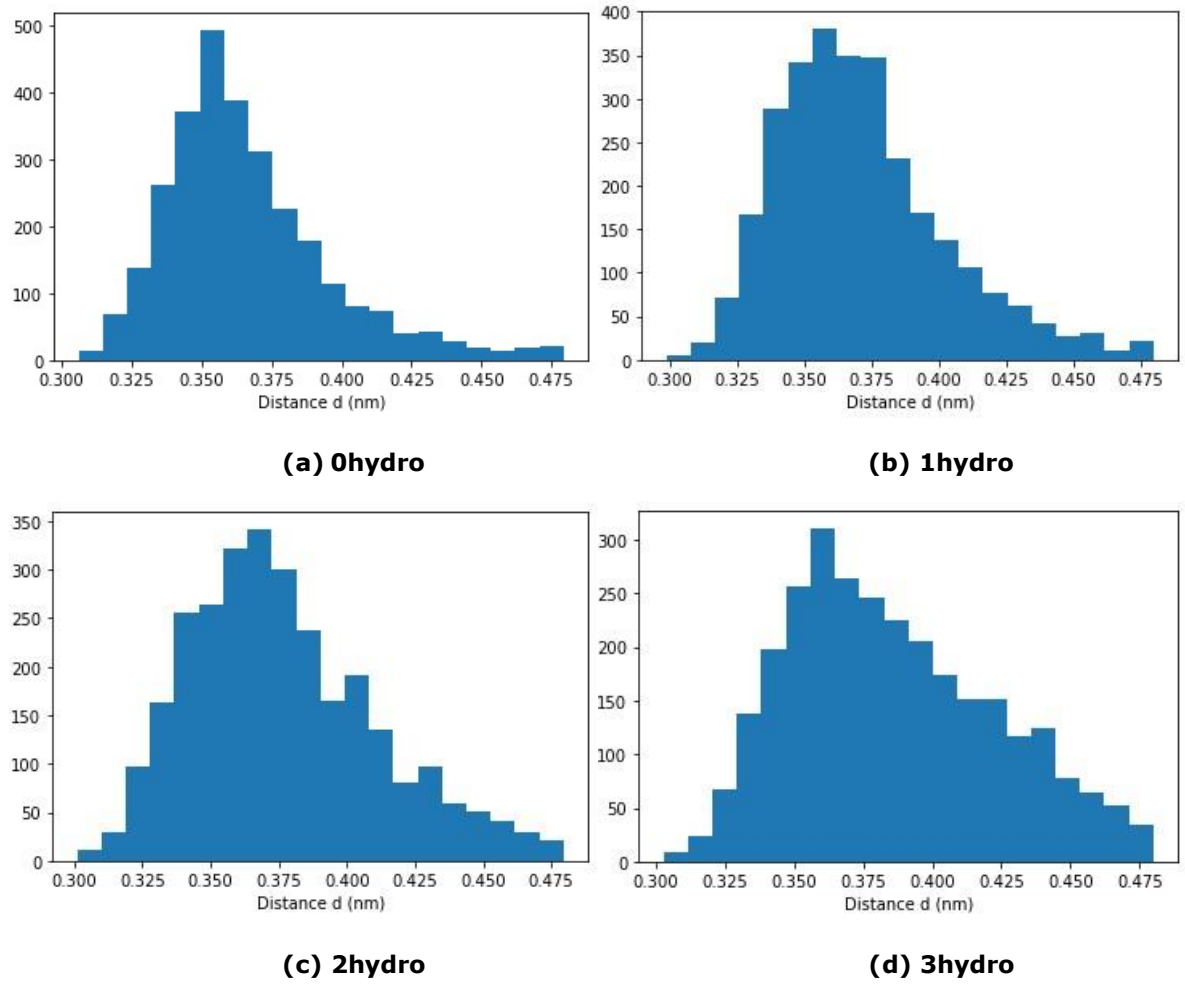

(a) 0hydro **(b) 1hydro**

(c) 2hydro **(d) 3hydro**

Figure 35 : Histogram of the distance d for each molecule, taking into account the 3 samples (i.e., 3000 distances calculated) and the cut-off

Molecule	0hydro	1hydro	2hydro	3hydro
d average (nm)	0,3663	0,3712	0,3766	0,3856
d standard deviation (nm)	0,0296	0,0315	0,0344	0,0372

Table 9 : d average and standard deviation values calculated with Python for each molecule, taking into account the 3 samples (i.e., 3000 distances calculated) and the cut-off

So, the extra hydroxy groups result in a slight increase of the angle α even the distribution stay very similar, and in a gradual increase of the length d while maintaining the same value of maximum probability (~3,6 nm).

3.4 Solvated Layer Study

In this part, the results about the hydroxy group influence on a solvated layer properties are presented and discussed. The layer width is still around 7 nm. The potential applications for an adhesive polymer and the boat hull coating improvement lead us to be interested more particularly in the behaviour of the material in an aqueous environment. We indeed wonder, comparatively to the simple layer, to what extent the structure and intermolecular interactions change with the additional hydroxy groups. The analyze is divided the same way as it is for the bulk study, in three topics: the hydrogen bonds, the energies and the structure arrangement. The hydrogen-bonds section will separate the case of bonds between the studied molecules and the case of bonds between water and the studied molecules.

3.4.1 Hydrogen-Bonds

First, Figure 36 and Figure 37 show the evolution of the number of H-bonds during the NVT equilibration of the solvated layer. As this simulation is an equilibration and the system was already somewhat in balance at the end of the previous simulated annealing, one can see that the numbers of H-bonds remains constant. However, as for the bulk and the layer, we notice that the differences between molecules are constant accross the simulation. The conclusion about the influence of the presence of hydroxy groups is the same as for the bulk and the layer; the number of H-bonds in the system increases with the number of hydroxy groups. As the hydroxy groups are likely to participate in a H-bond, the more hydroxy groups the system has, the more connections there are within the system.

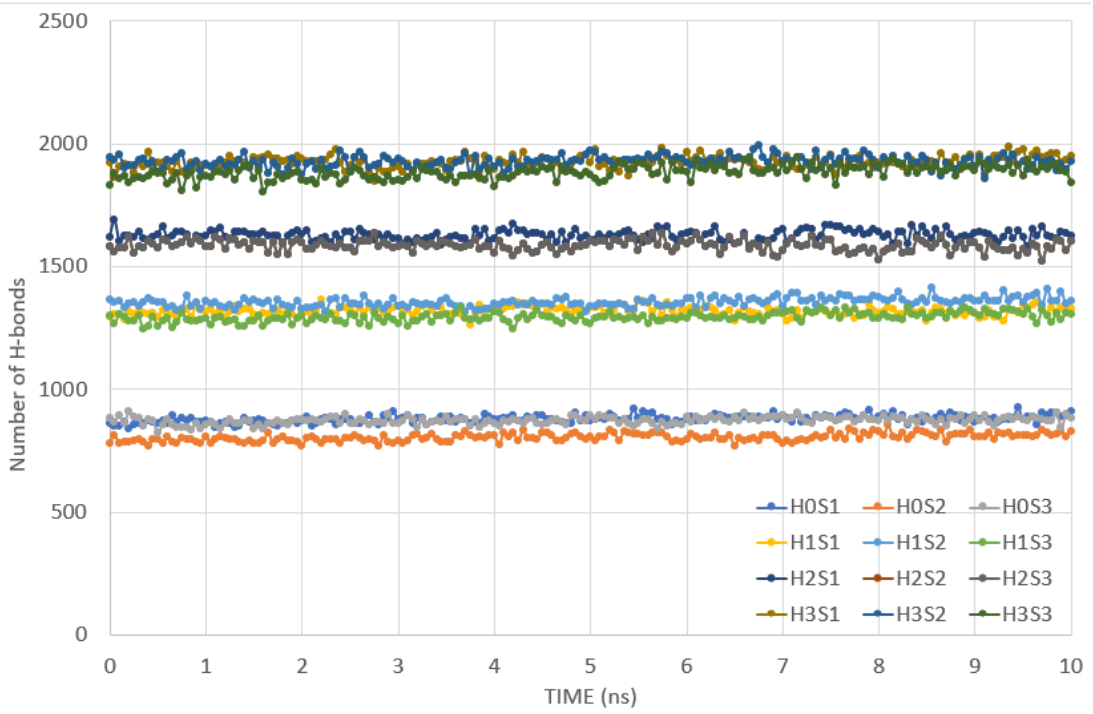

Figure 36 : Number of H-bonds, between *Xhydro* molecules, evolution during NVT equilibration for each sample

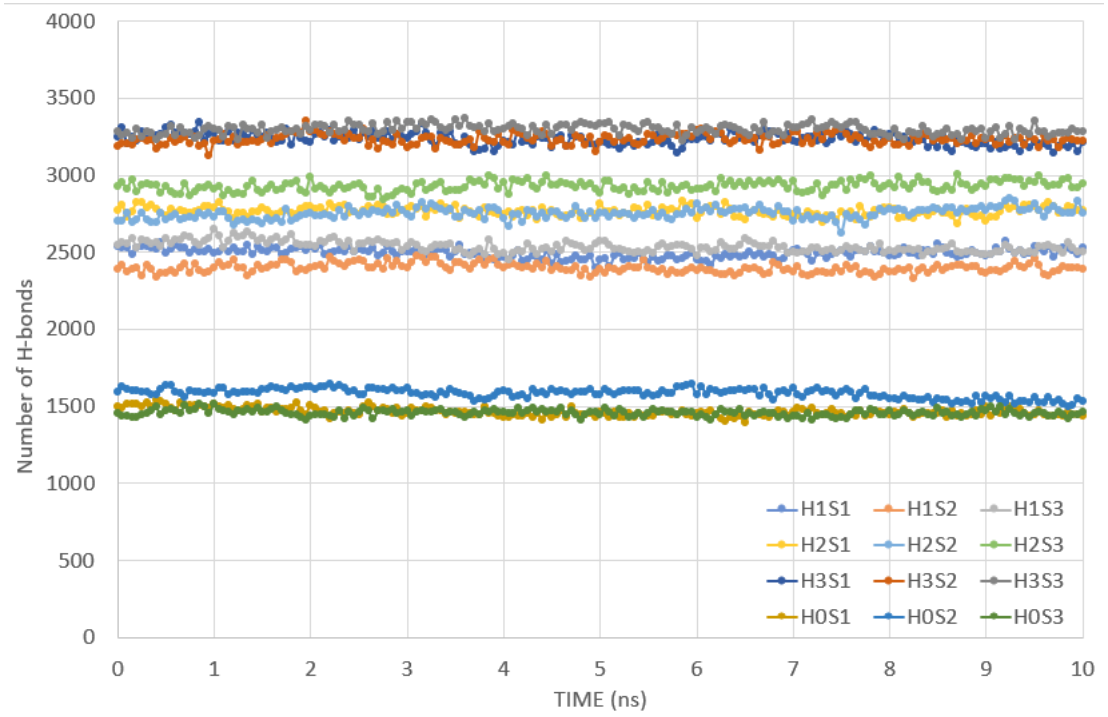

Figure 37 : Number of H-bonds, between *Xhydro* and water molecules, evolution during NVT equilibration for each sample

As shown in Figure 38 and Figure 39, the mean number of H-bonds for each molecule, in the end of the NVT equilibration. One may notice that the numbers of H-bonds between the studied molecules are lower than in the two previous cases. Indeed, the water has spread in the layer of material and occupy a part of the potential H-bonds. However, the additional hydroxy groups increase the number of bonds between the studied molecules and with the water. This result was expected because of the hydroxyl group is likely to interact with water. In both Figure 38 and Figure 39, the main gap is realized by the addition of the first hydroxy group : +471 and +1002 H-bonds from 0hydro to 1hydro against around +300 and +375 H-bonds from 1hydro to 2hydro and from 2hydro to 3hydro.

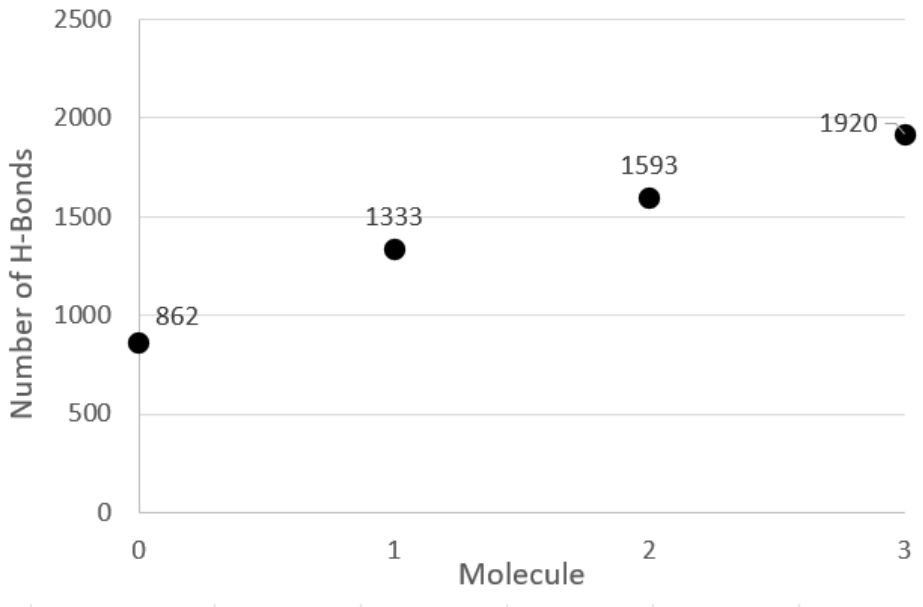

Figure 38 : Average number of H-bonds, between *Xhydro* molecules, per molecule-type during the last 0,5 ns of the simulation

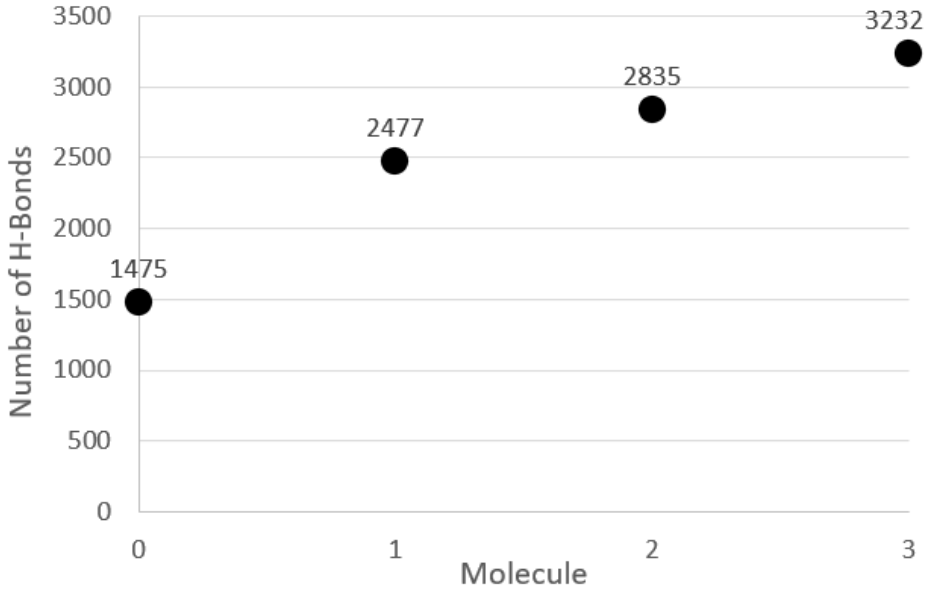

Figure 39 : Average number of H-bonds, between *Xhydro* and water molecules, per molecule-type during the last 0,5 ns of the simulation

The hydrogen bonding angles at the end of simulation are also collected and compared. The results are given into an average by molecule. For the third time, it appears in Figure 40 that, concerning the H-bonds between the studied molecules only, 3hydro has the tendancy of having less H-bonds between 5 to 15° and more above 20° than the others molecule. More samples would be required to confirm this effect caused by the third hydroxy group, meanwhile the three configurations give the same conclusion.

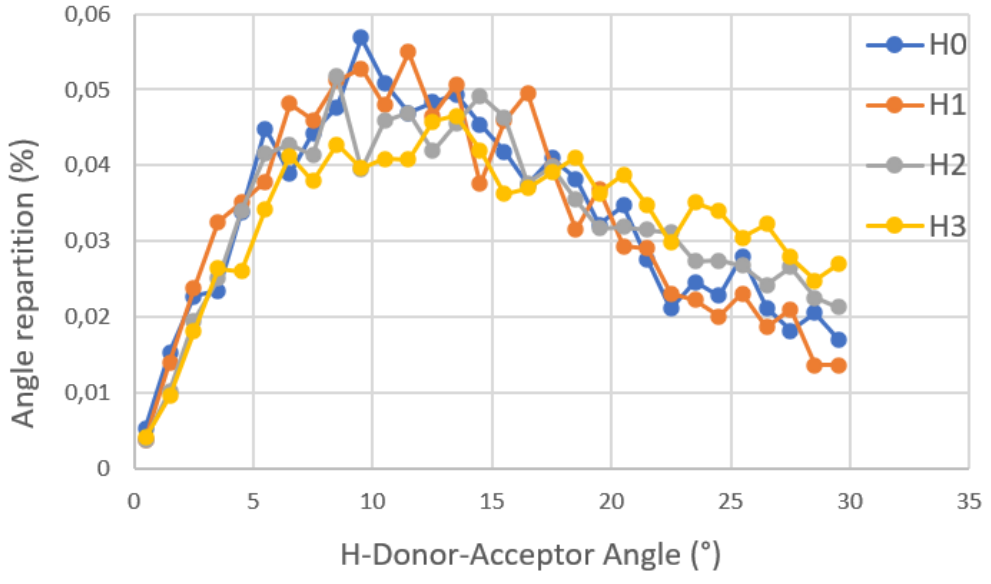

Figure 40 : Average repartition of the H-bond angle per molecule type, only bonds between *Xhydro molecules*

Figure 41 gives the same information but only for the H-bonds between the studied molecules and water molecules. The distributions are highly similar, mostly owing to the

mobility of water molecules at the first hydration layer [24]. The water molecules are able to feature the optimized hydrogen bonding angle on at the interface.

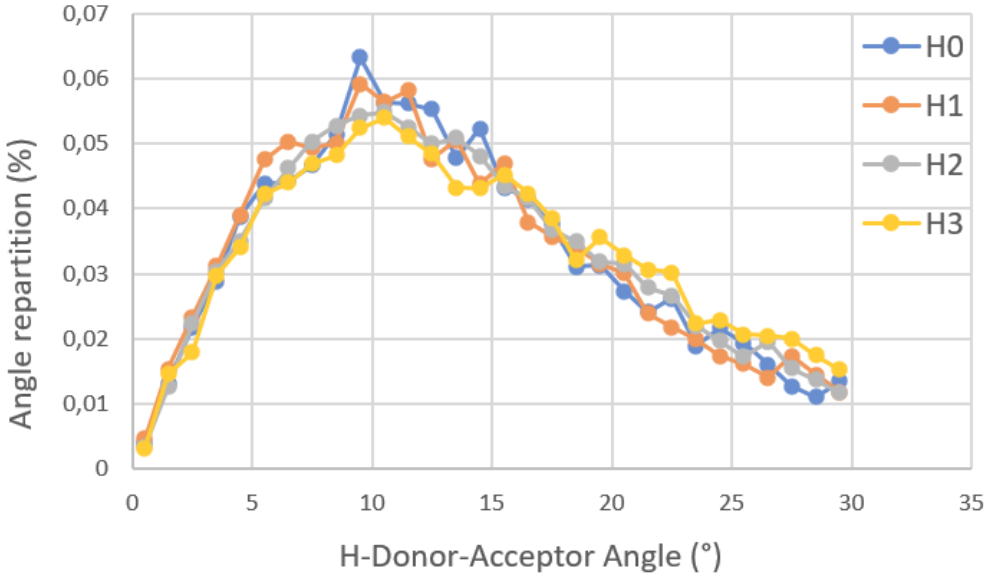

Figure 41 : Average repartition of the H-bond angle per molecule type, only bonds between *Xhydro* and water molecules

The H-bond length repartition by molecule is given in Figure 42 and Figure 43. Figure 42 shows that, in the case of the H-bonds among studied molecules only, 0hydro distingishes itself very clearly meanwhile the other molecules curves are pretty much the same. The conclusion doesn't change from the bulk and layer configurations. The addition of the hydroxyl groups on the sidechain, even only 1 in the 1hydro, makes shorter hydrogen bonds in the systems. The shorter the bonds are, the stronger. So this result indicates that the 1hydro, 2hydro and 3hydro should have overall stronger internal molecular interactions, and thus higher cohesive energy than that of 0hydro.

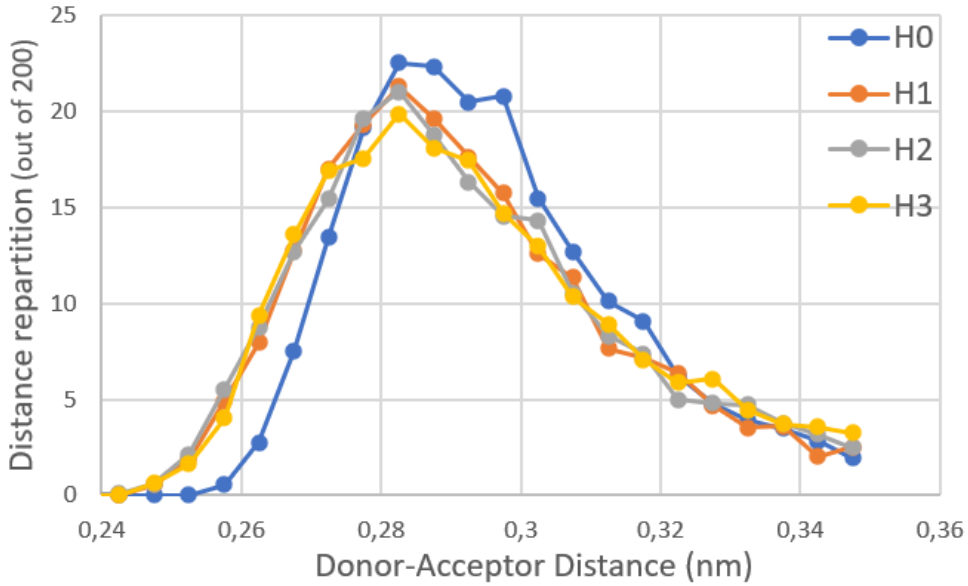

Figure 42 : Average repartition of the H-bond length per molecule type, only bonds between *Xhydro molecules*

In the other hand, Figure 43 demonstrates that the added hydroxy groups have no effect on the lenght of the H-bonds that occur between the studied molecules and the molecules

of water. Same as discussed above, the hydrogen bonding between the molecules with water molecules in the first hydration layer is the same in the systems, owing to the properties of the hydration layer.

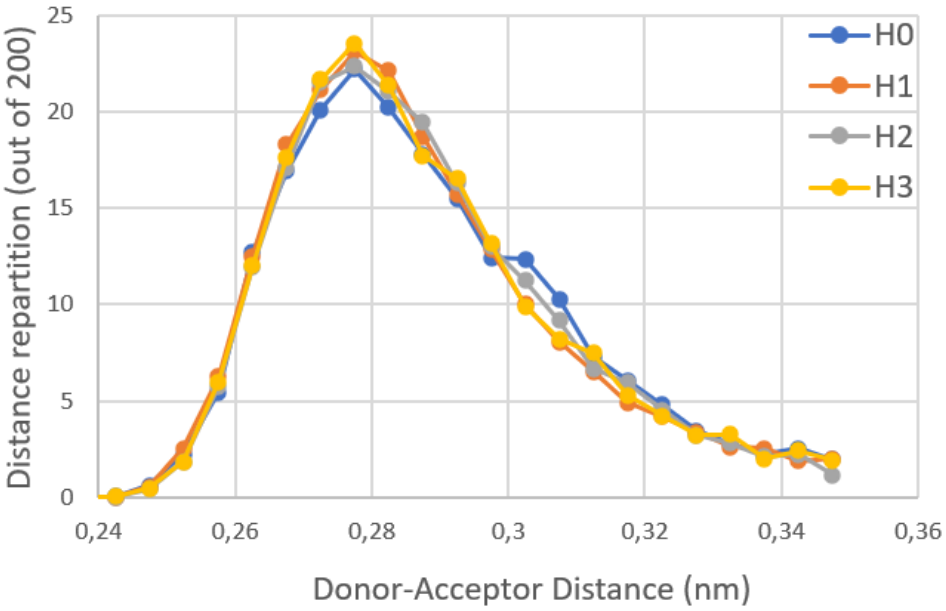

Figure 43 : Average repartition of the H-bond length per molecule type, only bonds between *Xhydro* and water molecules

In summary, concerning the H-bonds between the studied molecules, the conclusions are the following. The addition of the first hydroxy group in the system increases the number oh H-bonds more than the second and third ones. These numbers are lower than in the bulk and layer cases because of the water which also create H-bonds with the studied material, from the sides and inside. For the third time, the third added hydroxy group seems to increase the angle of hydrogen bonding. And finally, the h-bond's length distributions are the same for 1hydro, 2hydro and 3hydro, and towards shorter bonds than for 0hydro.

Concerning now the H-bonds between the studied molecules and the water, the more hydroxy groups are added the more hydrogen bonds are created with the water. The main difference is made by the first hydroxy group. However, no change is observed regarding the length and angle of hydrogen bonding.

3.4.2 Energy

As discussed above, the energetic properties of the system is an good indication of the system stability, which are also analysed for the layer systems. For each molecule-type, the potential energy, the bond energy, the Lennard-Jones potential and the Coulombic potential are given respectively in Figure 44, Figure 45, Figure 46 and Figure 47. It's recalled here that the a system is composed of one thousand molecules plsu the water, so the energies and potentials calculated are expected to be very different from the two previous configurations.

It can be seen in Figure 44 that the potential energy of the system decreases when the number of added hydroxy groups increases. The result was expected because of the increases of the number of hydrogen bonds found previously. The system is more stable with higher number of hydroxyl groups. However, it's noticeable that the decrease of the

system potential energy of the system is irregular regarding the addition of hydroxy groups. The most important energy change is obtained by the transition from 1hydro to 2hydro. The effects of the hydroxy group adding is the same as for the layer structure, simply the values are shifted by around -580 MJ/mol because of the presence of water.

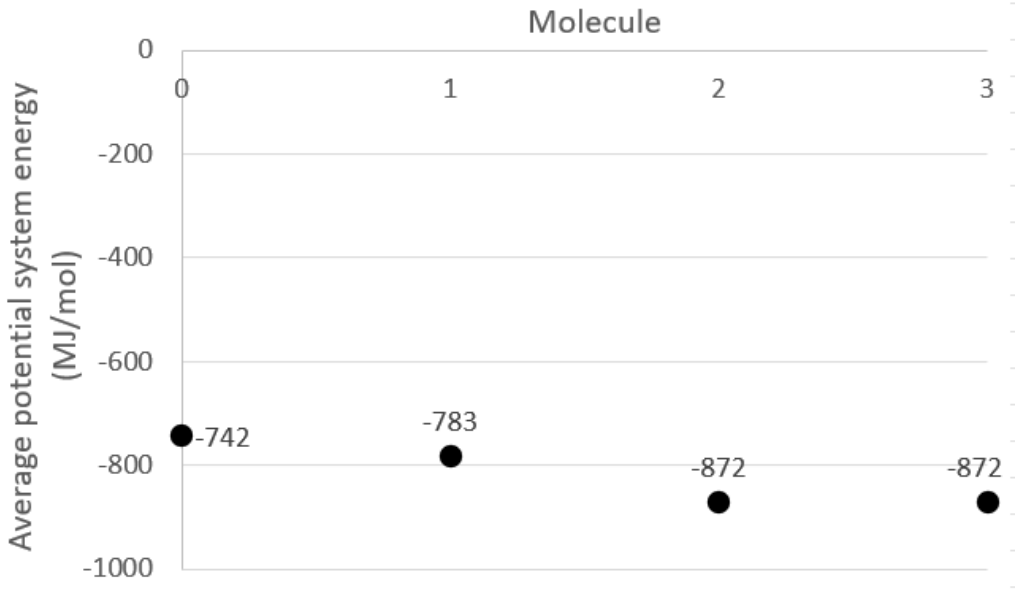

Figure 44 : Average potential system energy per molecule-type during the last 0,5 ns of the simulation

The bond energy shown Figure 45, called binding energy in physics and chemistry, represented the required energy to disassemble the system into individual parts. The higher is number of bonds in the systems, the tighter the atoms are bonded and the system in general. Therefore the increase of the bond energy following the increase of the number of hydroxy groups makes perfectly sense. Meanwhile it can be observed that increases seems to be linear and that the values are pretty close from those in the bulk and layer cases. The water does not act as a solvent to maintain the system together.

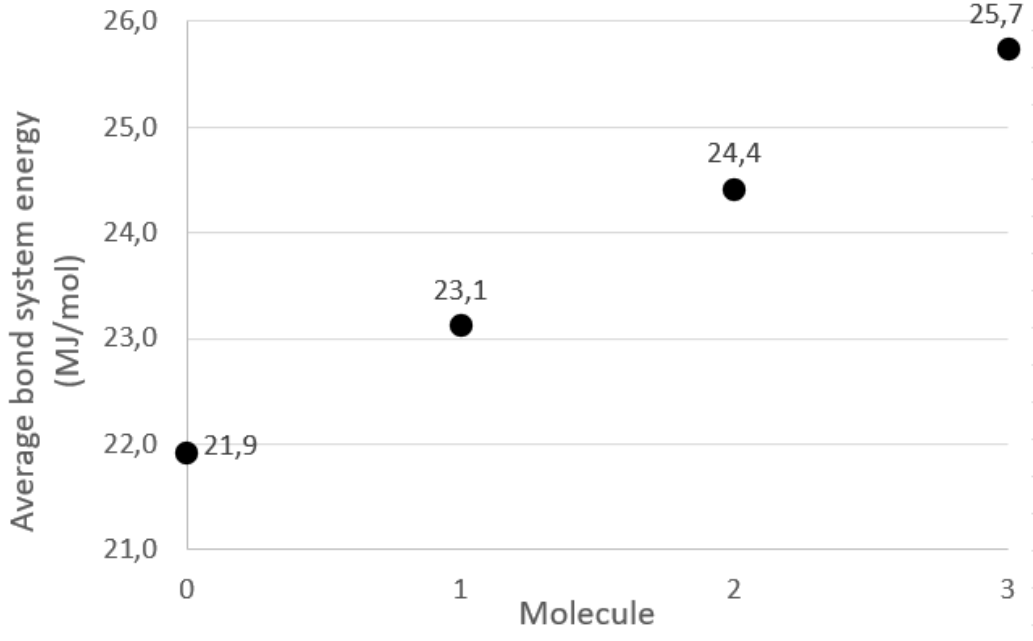

Figure 45 : Average bond system energy per molecule-type during the last 0,5 ns of the simulation

On the contrary, the evolutions of the Lennard-Jones and Coulombic potentials aren't consistent. The transitions from 0hydro to 1hydro and from 2hydro to 3hydro decrease the Lennard-Jones potential meanwhile the the transition from 1hydro to 2hydro increase the potential until the same value as 0hydro. The standard deviations for 1hydro and 2hydro are very high and so we can't suggest another conclusion than that the systems can evolve considerably regarding the Lennard-Jones potential.

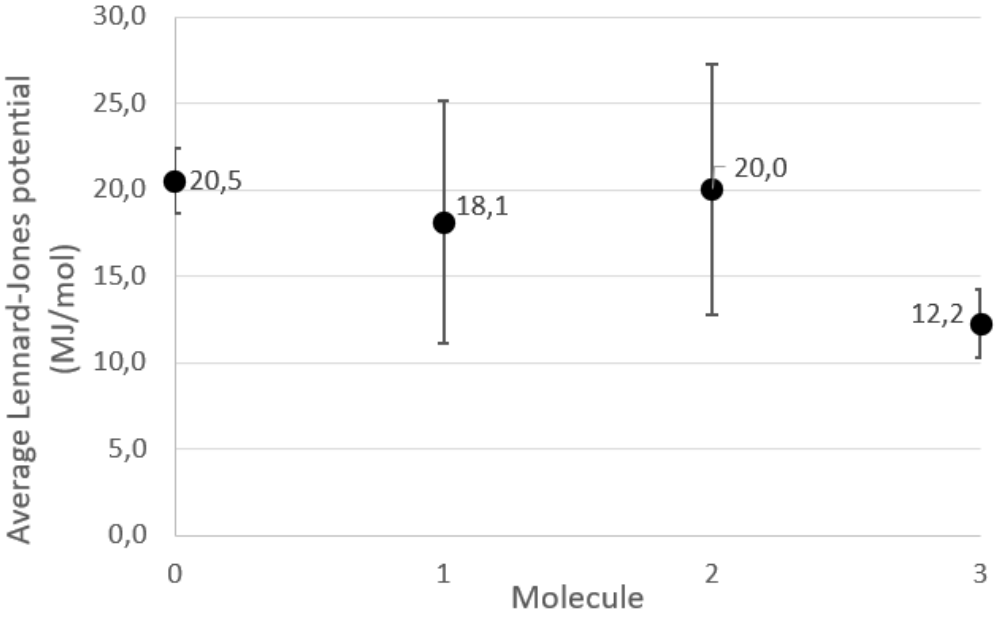

Figure 46 : Average system Lennard-Jones potential per molecule-type during the last 0,5 ns of the simulation. The error bars represent the average of the sample's standard deviation.

Regarding the Coulombic potential (Figure 47) a small evolution is first observed (-11 MJ/mol from 0hydro to 1hydro) and then an important one (-251 MJ/mol from 1hydro to 2hydro). The addition of the third hydroxy group creates a medium energy change (-73 MJ/mol). As such, the same conclusion could be draw as in the bulk and the layer systems. The evolution of the Coulombic potential with the additional hydroxy groups is the same as for the two previous structures, again the values are simply shifted because they consider the potential of the water.

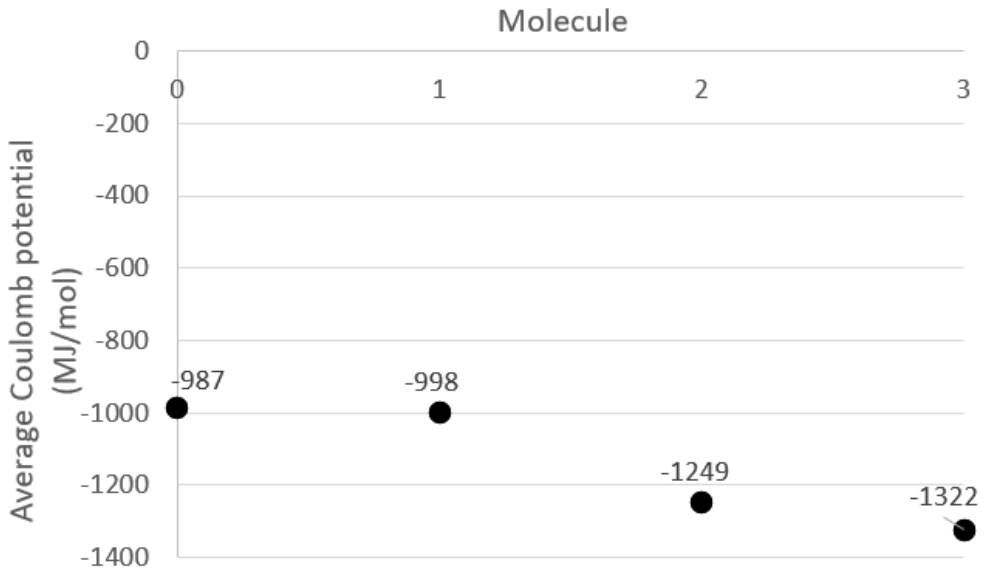

Figure 47 : Average system Coulombic potential per molecule-type during the last 0,5 ns of the simulation

Regarding the energies, the conclusions made previously can be made again. Indeed, the presence of the water shifts all the system potential, Lennard-Jones potential and Coulombic potential values. However, the bond system energy remains the same because the water does not help pulling the system together.

3.4.3 Python Code Analyzis

Finally we stop being interested in inter and intra molecular interactions but rather in how the molecules arrange themselves in relation to each other in the layer. So the parameters d and α described in Introduction are used for the analyzis.

Table 10 presents the number of remaining values after the application of the cut-off. Between 100 and 250 values are deleted in each case, the vast majority of our rings are therefore considered to be interacting.

Molecule type	0hydro	1hydro	2hydro	3hydro
Number values d and α remaining after the cut-off 0,48 nm	2895	2829	2817	2786

Table 10 : Cut-off effect among the 3000 d and α calculated

Figure 48 shows for each molecule-type the distribution of the angles for the π-π interactions detected in the final configuration of the system in the end of the NVT equilibration. Besides, the average angles and standard deviations are gathered in Table 11. The standard deviation is important and it seems that there is not one strict favorable conformation. The average angle results confirms in a way the conclusion of previous studies [17] saying that the T-shape conformation ($\alpha \approx {}^{\pi}/_{2}$) could be the most favorable arrangement for our molecules. Meanwhile it can be seen that for the molecules with added hydroxy groups, the probability density for high angles is higher than for 0hydro, particularly in the case of 1hydro for which the average α reaches 1,6738 rad. It could be explained by the polarization of the ring by the oxygen atoms, which leads to more sandwich and parallel-displaced conformations in the bulk. Indeed previous studies' [17]

rule number 5 says that a π-deficient atom in a face-to-face geometry could lead to a favourable interaction with a neutral or weakly polarized site.

In the layer configuration the main change may be from the transition from 0hydro to 1hydro meanwhile the next additions are steps backwards. The mean value change with the additional hydroxy groups but also the shapes of the distribution. The values for 1hydro, 2hydro and 3hydro are very close from those for the layer structure, meanwhile the value corresponding to 0hydro is lower with the water.

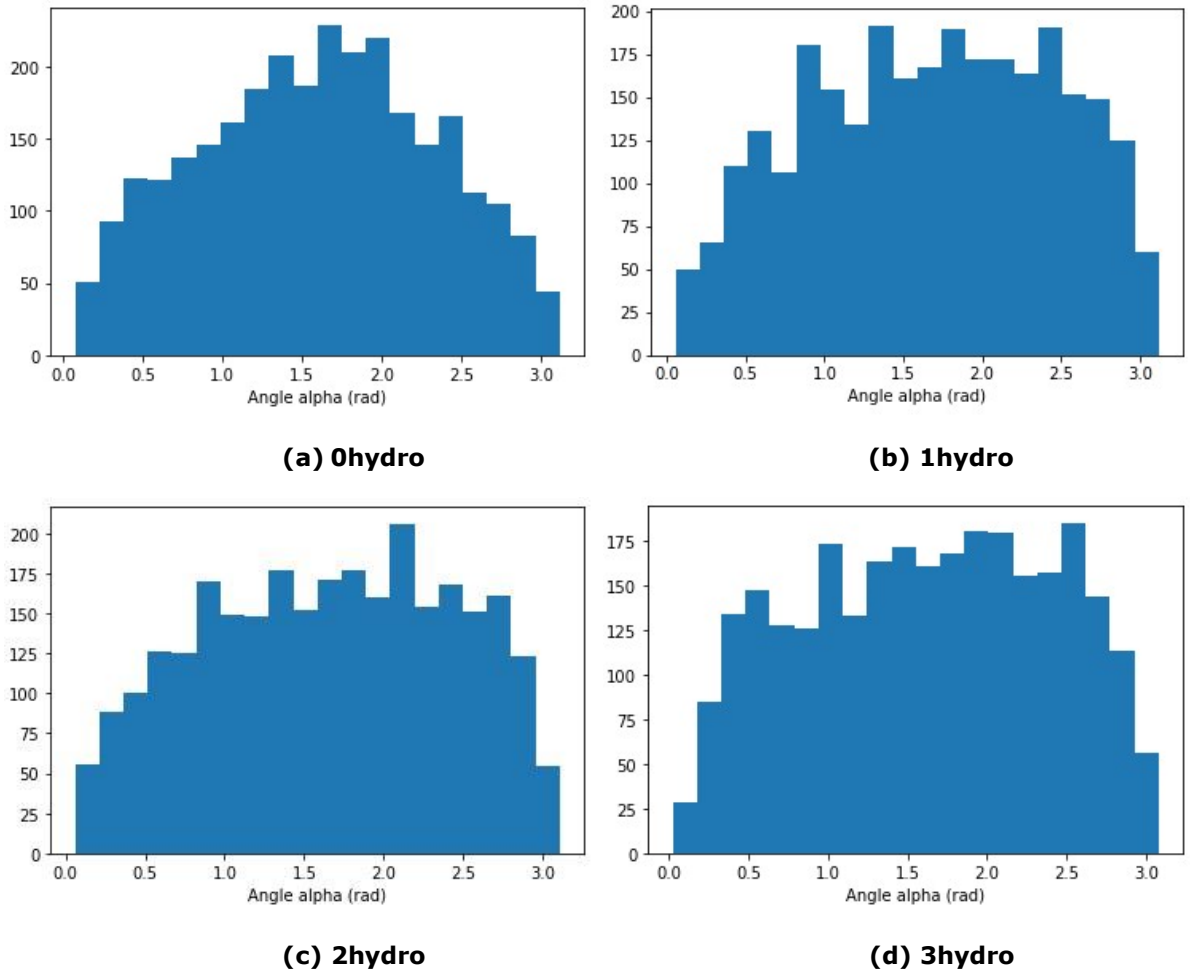

(a) 0hydro **(b) 1hydro**

(c) 2hydro **(d) 3hydro**

Figure 48 : Histogram of the angle α for each molecule, taking into account the 3 samples (i.e., 3000 angles calculated) and the cut-off

Molecule	0hydro	1hydro	2hydro	3hydro
α average (rad)	1,5920	1,6738	1,6551	1,6188
α standard deviation (rad)	0,7314	0,7734	0,7775	0,7790

Table 11 : α average and standard deviation values calculated with Python for each molecule, taking into account the 3 samples (i.e., 3000 angles calculated) and the cut-off

As for the bulk configuration, the Figure 49 demonstrates that the addition of the oxygen atoms to form hydroxy groups lenghtens the distance d between the rings. It can be explain by the fact that in the T-shape conformation for example, the oxygen is one more atom between the two carbons we use to calculate the inter-molecular distance d, but also by

the change of the molecule's moment. Table 12 makes clear the progressive increase of the distance d with the additions of hydroxy group.

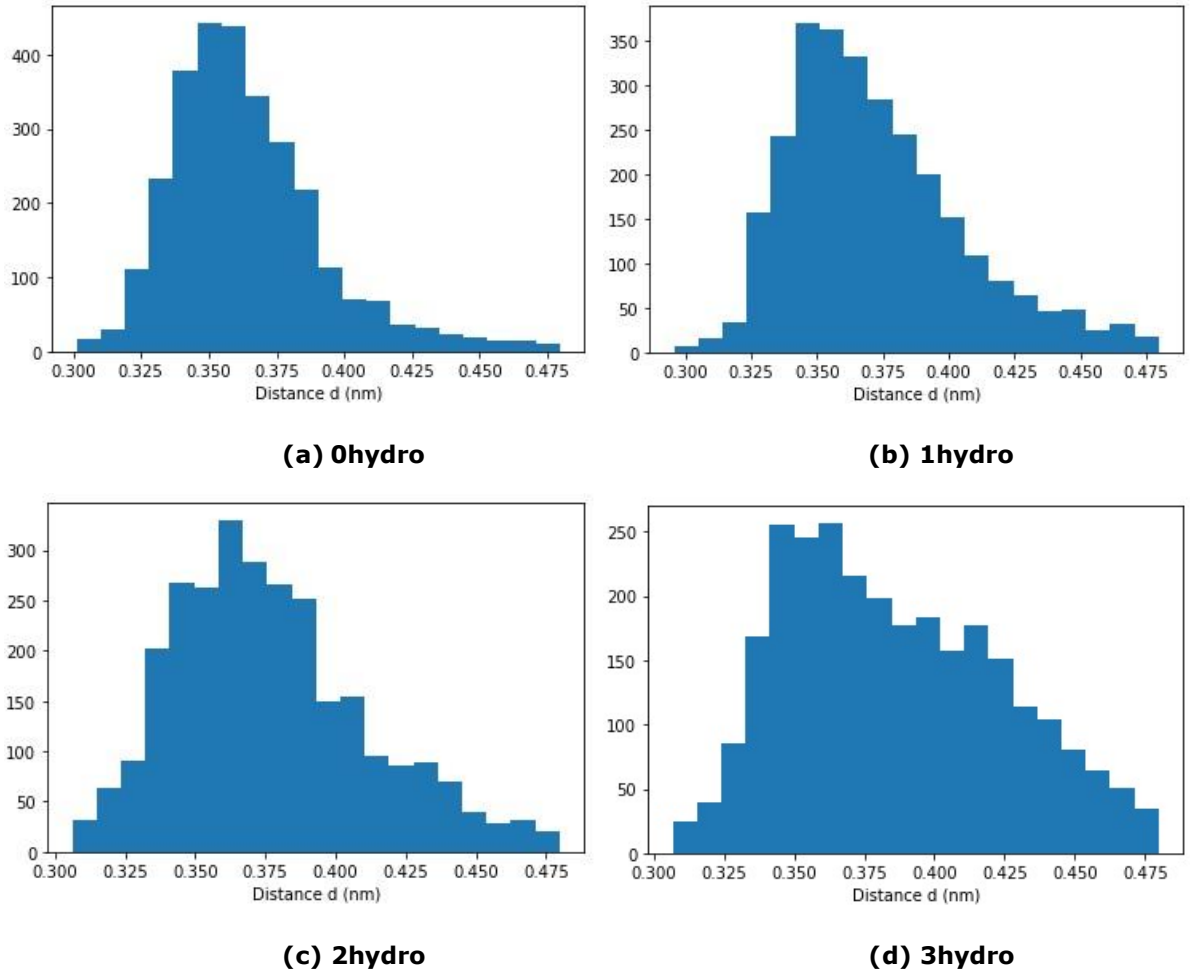

(a) 0hydro **(b) 1hydro**

(c) 2hydro **(d) 3hydro**

Figure 49 : Histogram of the distance d for each molecule, taking into account the 3 samples (i.e., 3000 distances calculated) and the cut-off

Molecule	0hydro	1hydro	2hydro	3hydro
d average (nm)	0,3640	0,3723	0,3766	0,3856
d standard deviation (nm)	0,0282	0,0329	0,0343	0,0384

Table 12 : d average and standard deviation values calculated with Python for each molecule, taking into account the 3 samples (i.e., 3000 distances calculated) and the cut-off

So, the extra hydroxy groups result in a slight increase of the angle α even the distribution stay very similar, and in a gradual increase of the length d while maintaining the same value of maximum probability (~3,6 nm).

4 Conclusion and Outlook

The study of DOPA derivatives materials has shown that the hydroxyl groups added on the benzene ring play the same role whether the structure is a bulk, a layer or a solvated layer. Hydroxyl groups actively participate in forming H-bonds, especially the first added hydroxyl group leads to the main increase of number of H-bonds. Besides, they shorten the length of the H-bonds but do not impact the H-bonds angles. This work highlights the role molecular interactions played by the hydroxyl groups, increasing the bonding energy of the systems and decreasing the Lennard-Jones and Coulombic potentials and the global potential energy. It's interesting to note that those decreases are irregular and that the most important change is done by the addition of the second hydroxyl group on the benzene ring. Finally, the hydroxyl groups have an impact on the conformation of the DOPA derivatives, shortening the distance inter-benzenes and modifying the angles formed by the interacting benzenes.

The study of DOPA derivatives with Molecular Dynamics simulations highlighted the effects of hydroxyl groups on inter-molecule interactions, while the work carried out in Python revealed their impact on the geometry of inter-molecule interactions. Those results allow a better understanding of the key role played by hydroxyl groups in MFP-like adhesive molecules.

Each molecule in each of the structures was simulated three times independently. More samples would have enabled better probabilistic reliability and therefore conclusions on the lighter effects of hydroxyl groups. However, this work focus on the side chain properties by the simulations of systems composed by monomers. The next step would be the modelling of bigger polymer chain in order to confirm or precise the hydroxyl groups role in experimental systems.

References

1. Kamino, K., *Underwater adhesive of marine organisms as the vital link between biological science and material science.* Marine Biotechnology, 2008. **10**: p. 111-121.
2. Lu, Q., et al., *Adhesion of mussel foot proteins to different substrate surfaces.* Journal of The Royal Society Interface, 2013. **10**(79): p. 20120759.
3. Kord Forooshani, P. and B.P. Lee, *Recent approaches in designing bioadhesive materials inspired by mussel adhesive protein.* Journal of Polymer Science Part A: Polymer Chemistry, 2017. **55**(1): p. 9-33.
4. Dalsin, J.L. and P.B. Messersmith, *Bioinspired antifouling polymers.* Materials today, 2005. **8**(9): p. 38-46.
5. Sun, J., et al., *Bioengineered Protein‐based Adhesives for Biomedical Applications.* Chemistry–A European Journal, 2022. **28**(1): p. e202102902.
6. Frontera, A., D. Quinonero, and P.M. Deya, *Cation–π and anion–π interactions.* Wiley Interdisciplinary Reviews: Computational Molecular Science, 2011. **1**(3): p. 440-459.
7. Badar, M.S., et al., *Molecular dynamics simulations: concept, methods, and applications*, in *Transdisciplinarity*. 2022, Springer. p. 131-151.
8. Chang, C.-E., W. Chen, and M.K. Gilson, *Evaluating the accuracy of the quasiharmonic approximation.* Journal of Chemical Theory and Computation, 2005. **1**(5): p. 1017-1028.
9. Abraham, M.J., et al., *GROMACS: High performance molecular simulations through multi-level parallelism from laptops to supercomputers.* SoftwareX, 2015. **1**: p. 19-25.
10. Ponder, J.W. and D.A. Case, *Force fields for protein simulations.* Advances in protein chemistry, 2003. **66**: p. 27-85.
11. Cuadros, F., I. Cachadiña, and W. Ahumada, *Determination of Lennard-Jones interaction parameters using a new procedure.* Molecular engineering, 1996. **6**: p. 319-325.
12. Gilli, G. and P. Gilli, *The nature of the hydrogen bond: outline of a comprehensive hydrogen bond theory*. Vol. 23. 2009: Oxford university press.
13. Sharma, D., et al., *Solubility enhancement–eminent role in poorly soluble drugs.* Research Journal of Pharmacy and Technology, 2009. **2**(2): p. 220-224.
14. Gautam, B., *Energy Minimization.* Homology Molecular Modeling-Perspectives and Applications, 2020.
15. Lindahl, A., S. Hess, and D. van der Spoel, *GROMACS 2020 Source code.* Zenodo: Geneve, Switzerland, 2020.
16. Sedó, J., et al., *Catechol‐based biomimetic functional materials.* Advanced Materials, 2013. **25**(5): p. 653-701.
17. Hunter, C.A. and J.K. Sanders, *The nature of. pi.-. pi. interactions.* Journal of the American Chemical Society, 1990. **112**(14): p. 5525-5534.
18. Thakuria, R., N.K. Nath, and B.K. Saha, *The nature and applications of π–π interactions: a perspective.* Crystal Growth & Design, 2019. **19**(2): p. 523-528.
19. Sinnokrot, M.O. and C.D. Sherrill, *Substituent effects in π− π interactions: sandwich and T-shaped configurations.* Journal of the American Chemical Society, 2004. **126**(24): p. 7690-7697.
20. Hunter, C.A., J. Singh, and J.M. Thornton, *π-π interactions: the geometry and energetics of phenylalanine-phenylalanine interactions in proteins.* Journal of molecular biology, 1991. **218**(4): p. 837-846.
21. Melchionna, S., G. Ciccotti, and B. Lee Holian, *Hoover NPT dynamics for systems varying in shape and size.* Molecular Physics, 1993. **78**(3): p. 533-544.
22. Siu, S.W., K. Pluhackova, and R.A. Böckmann, *Optimization of the OPLS-AA force field for long hydrocarbons.* Journal of Chemical theory and Computation, 2012. **8**(4): p. 1459-1470.
23. Bilotto, P., et al., *Adhesive properties of adsorbed layers of two recombinant mussel foot proteins with different levels of DOPA and tyrosine.* Langmuir, 2019. **35**(48): p. 15481-15490.
24. Bagchi, B., *Water dynamics in the hydration layer around proteins and micelles.* Chemical Reviews, 2005. **105**(9): p. 3197-3219.

Appendices

Appendix 1: Numbers of potential H-bonds in the bulk structure

Appendix 2: Numbers of potential H-bonds in the layer structure

Appendix 3: Numbers of potential H-bonds in the solvated layer structure

Appendix 1:

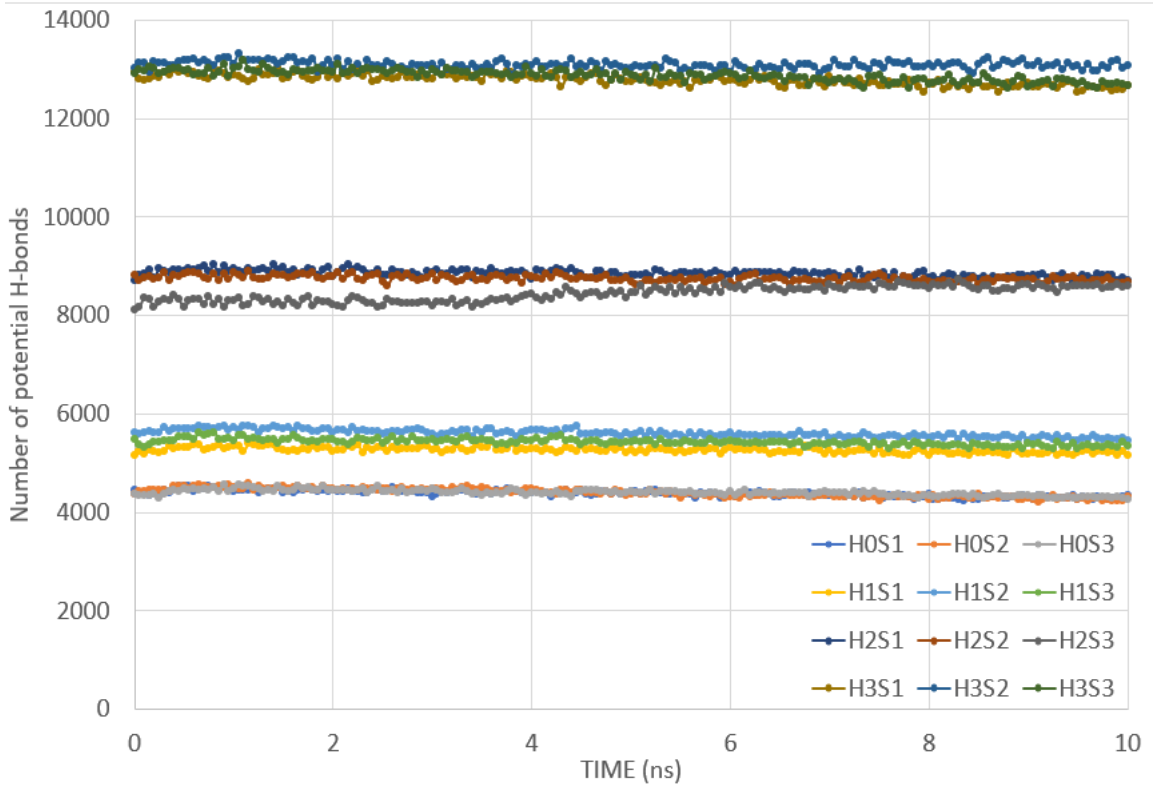

Figure 50 : Number of potential H-bonds evolution during simulated annealing for each sample in the bulk configuration

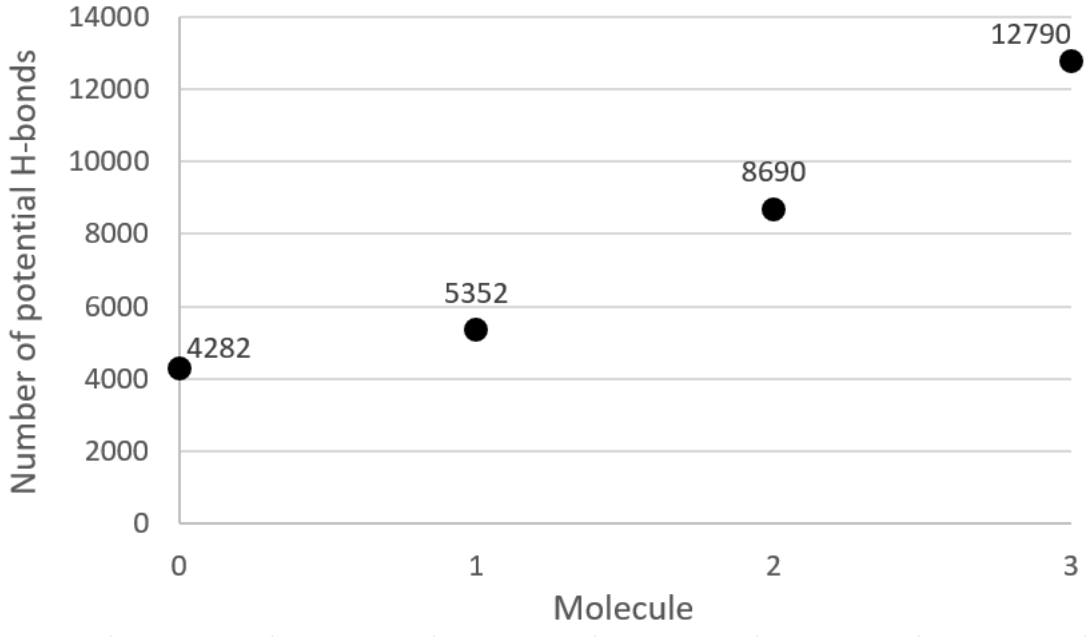

Figure 51 : Average number of potential H-bonds per molecule-type during the last 0,5 ns of the simulation (equilibrium) in the bulk configuration

Appendix 2:

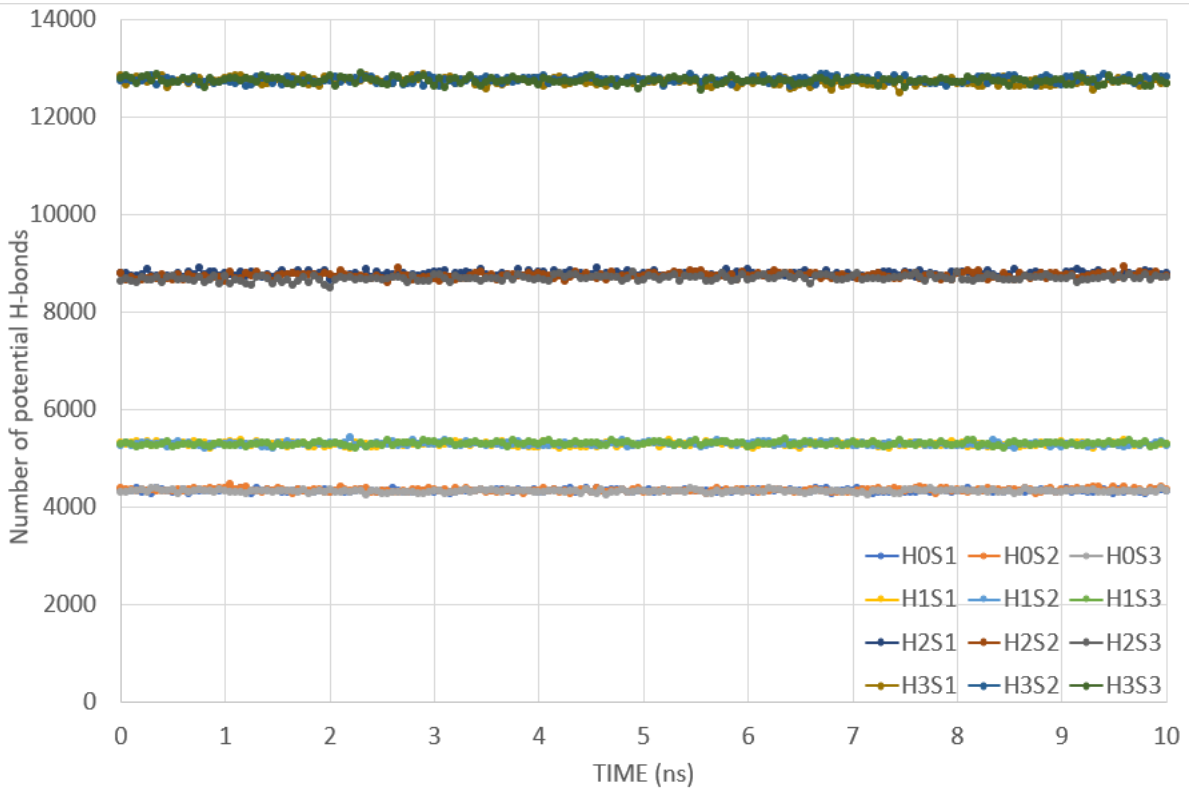

Figure 52 : Number of potential H-bonds evolution during NVT equilibration for each sample in the layer configuration

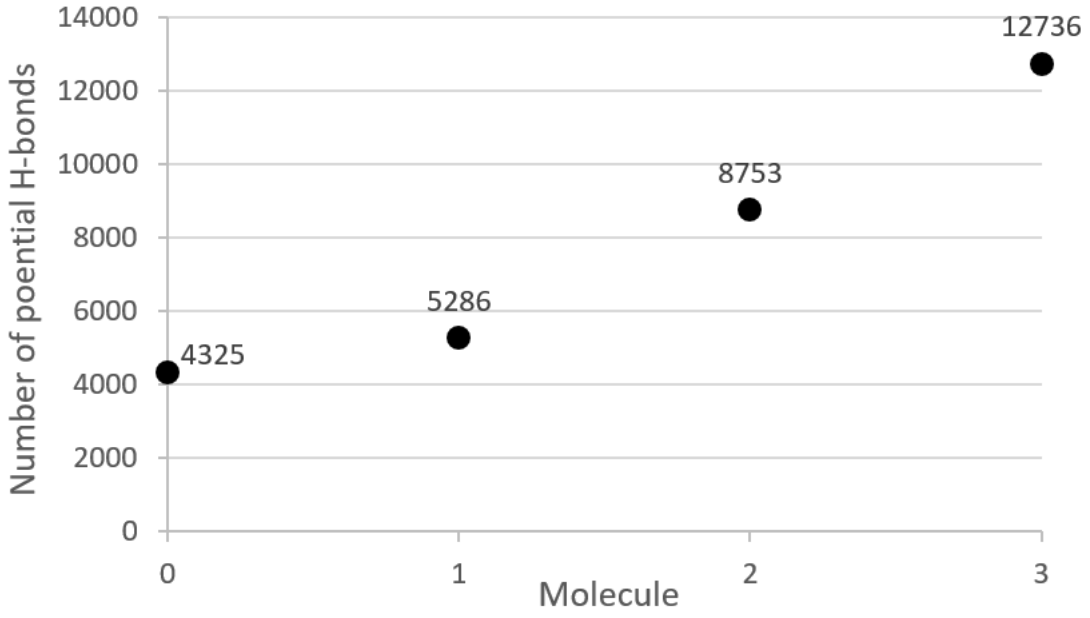

Figure 53 : Average number of potential H-bonds per molecule-type during the last 0,5 ns of the simulation (equilibrium) in the layer configuration

Appendix 3:

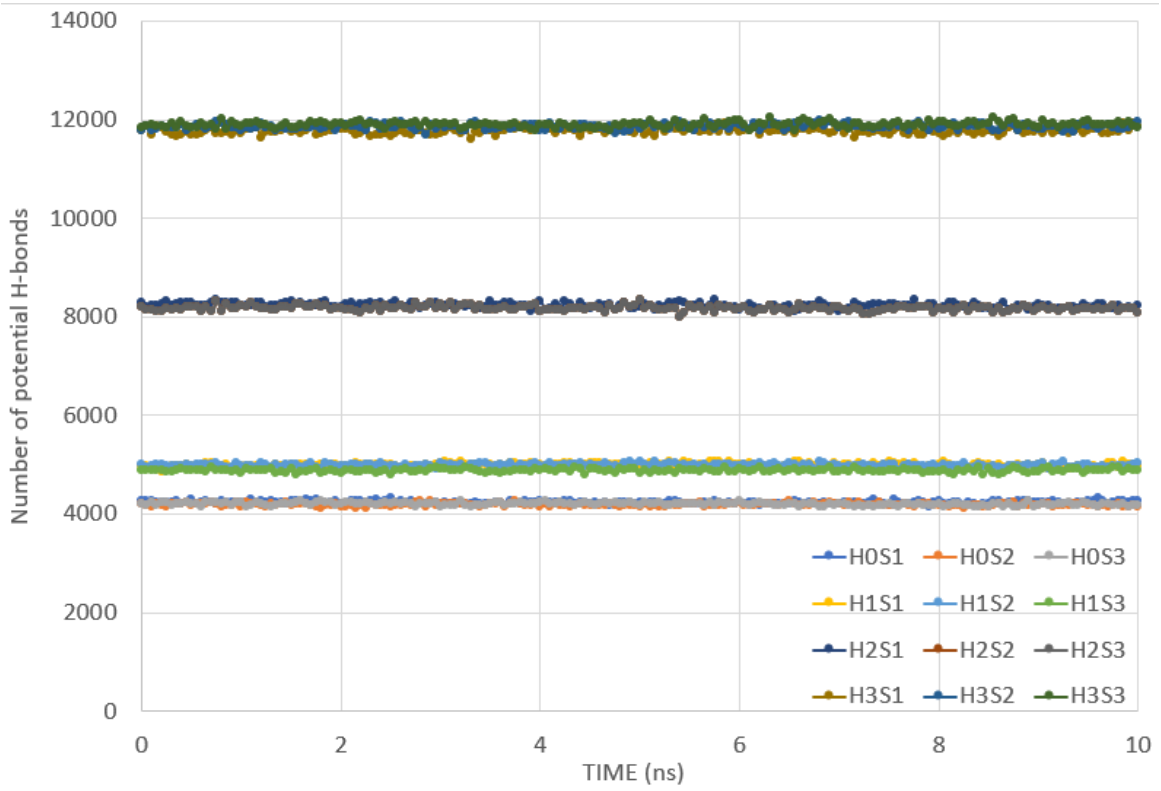

Figure 54 : Number of potential H-bonds, between studied molecules only, evolution during NVT equilibration for each sample in the solvated layer configuration

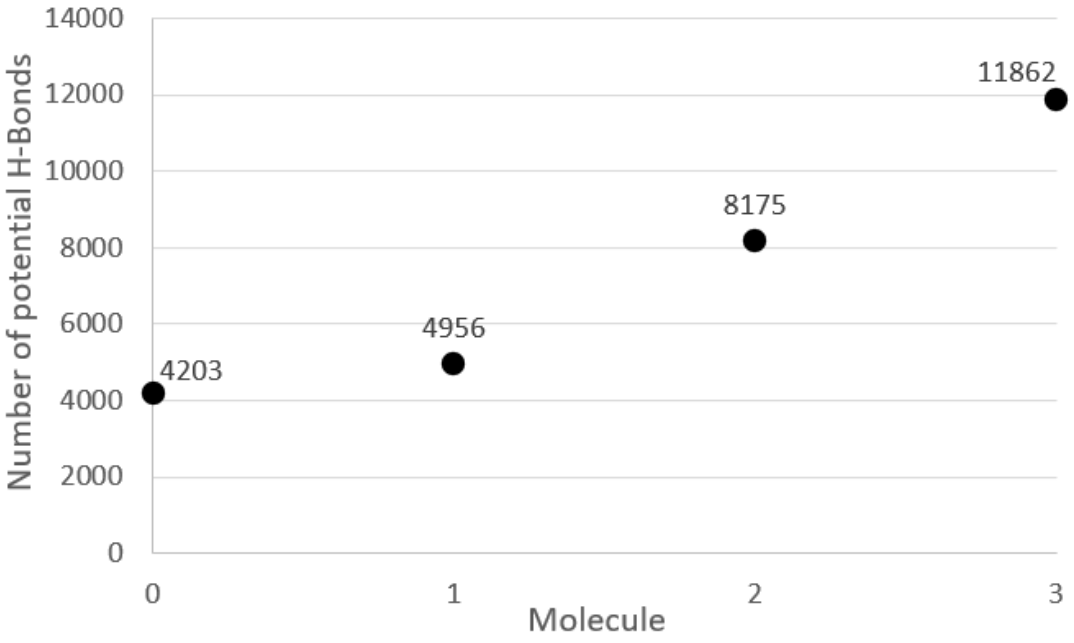

Figure 55 : Average number of potential H-bonds, between studied molecules only, per molecule-type during the last 0,5 ns of the simulation (equilibrium) in the solvated layer configuration

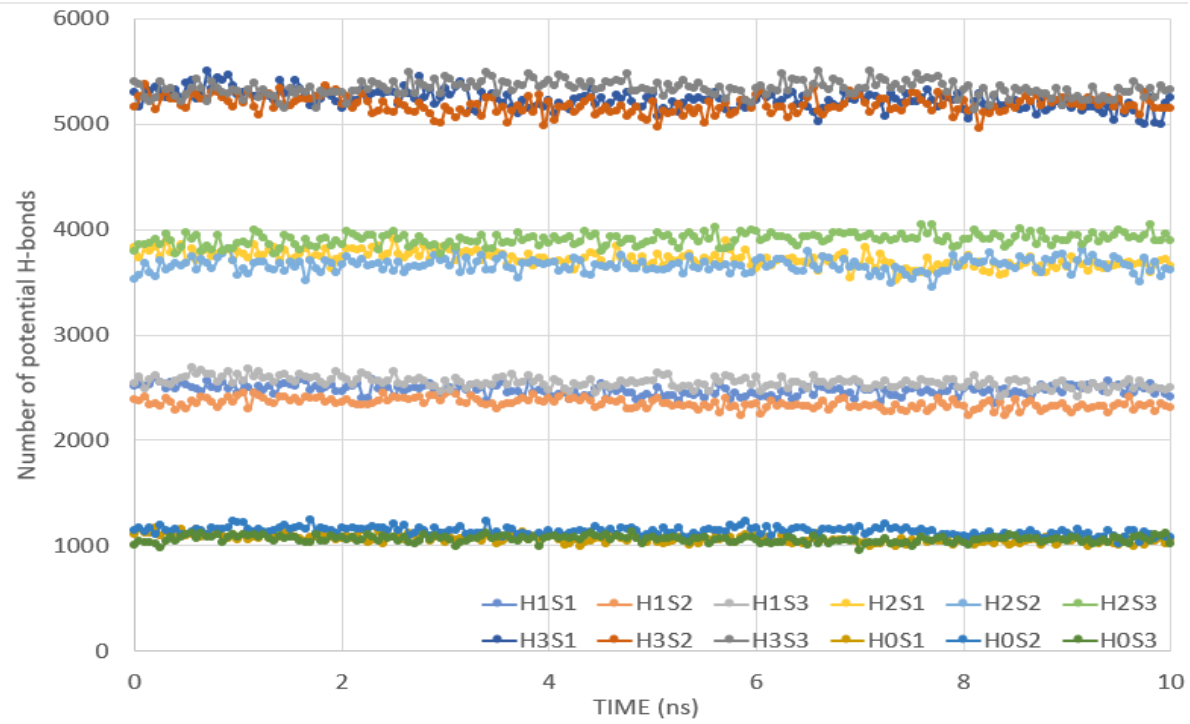

Figure 56: Number of potential H-bonds, between studied molecules and water, evolution during NVT equilibration for each sample in the solvated layer configuration

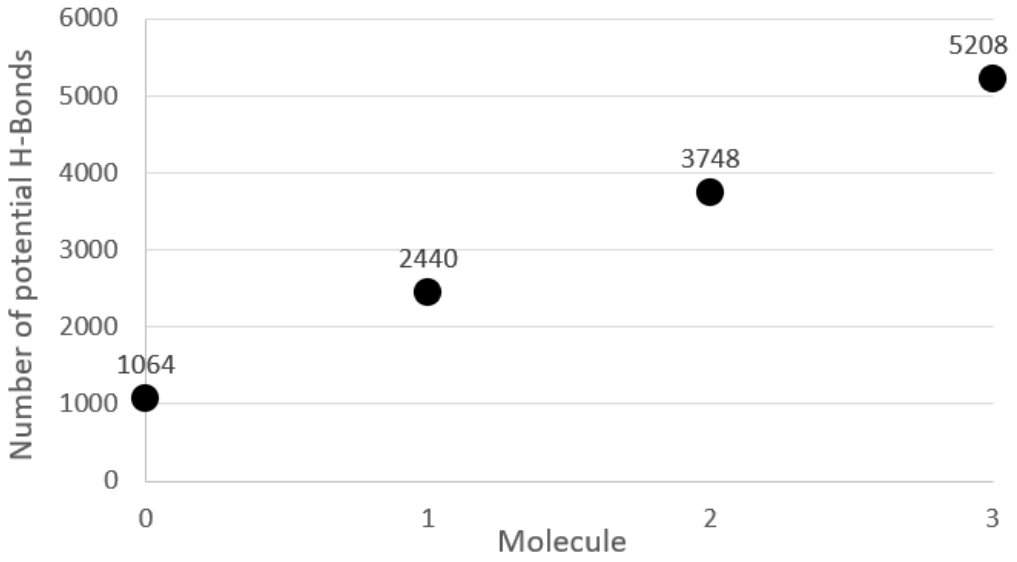

Figure 57: Average number of potential H-bonds, between studied molecules and water, per molecule-type during the last 0,5 ns of the simulation (equilibrium) in the solvated layer configuration

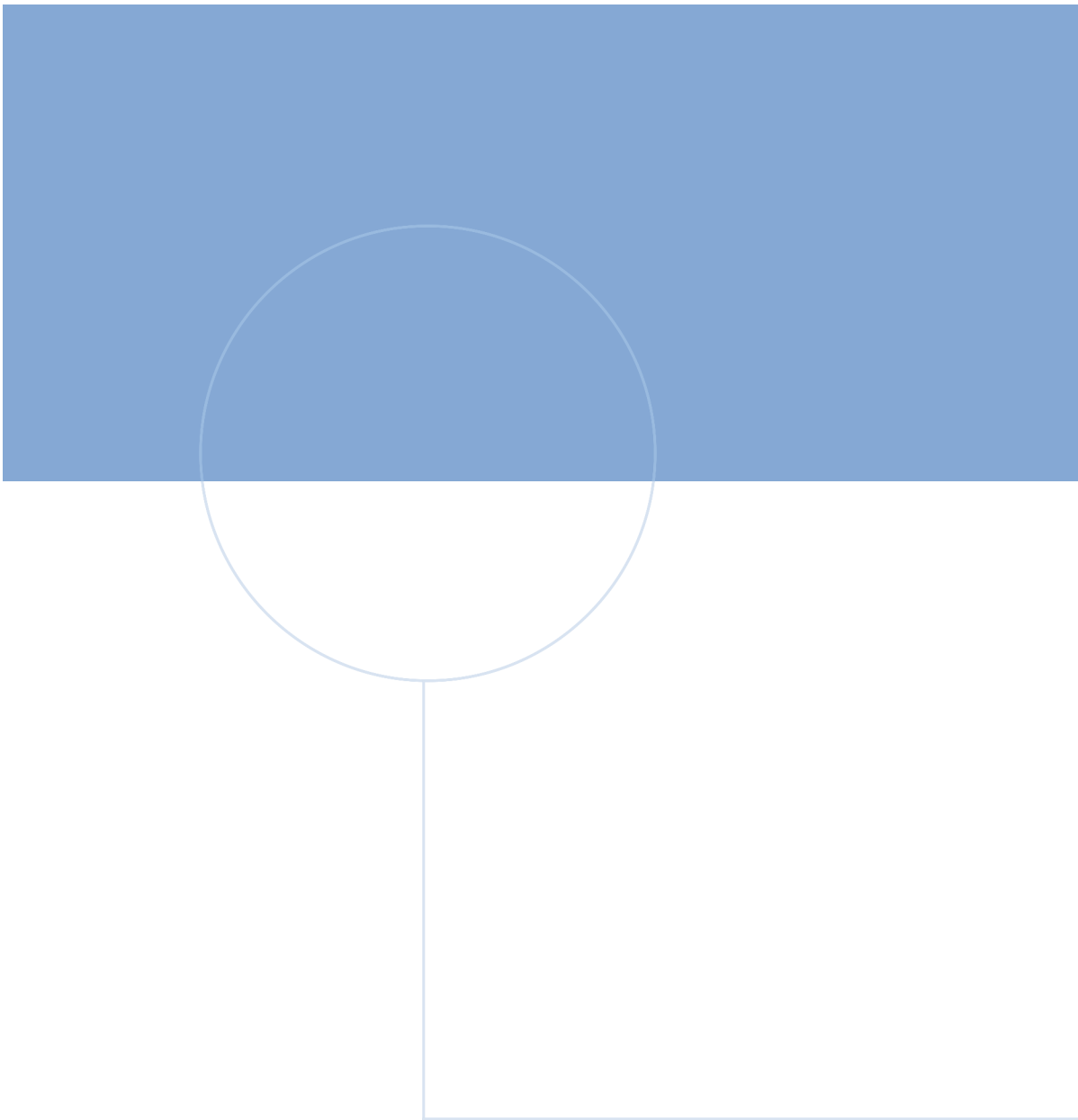

NTNU

Norwegian University of
Science and Technology